Coordination Chemistry Reviews 253 (2009) 2872–2890

Contents lists available at ScienceDirect

Coordination Chemistry Reviews

journal homepage: www.elsevier.com/locate/ccr

Review

Stabilization and immobilization of polyoxometalates in porous coordination polymers through host–guest interactions

Rongmin Yu [a], Xiao-Fei Kuang [a], Xiao-Yuan Wu [a], Can-Zhong Lu [a,*], James P. Donahue [b]

[a] The State Key Laboratory of Structural Chemistry, Fujian Institute of Research on the Structure of Matter, The Chinese Academy of Sciences, Fuzhou, Fujian, 350002, PR China
[b] Department of Chemistry, Tulane University, 6400 Freret Street, New Orleans, LA 70118, USA

Contents

ARTICLE INFO

Article history:
Received 1 April 2009
Accepted 8 July 2009
Available online 16 July 2009

Dedicated to Prof. Xintao Wu for his 70th birthday.

Keywords:
Polyoxometalates
Host–guest
Inorganic–organic composite
Keggin structure
Coordination polymer
Magnetic properties

ABSTRACT

The stabilization and immobilization of polyoxometalates (POMs) through the formation of POM-containing coordination polymers is one of the more attractive areas of supramolecular chemistry and POM materials. Owing to their various structural topologies and chemical compositions, which endow them with tunable shape, size and high negative charges, POMs are remarkably versatile building blocks in the construction of coordination supramolecules. Frequently, POMs act as anionic templates to build three-dimensional metal organic frameworks. In this review, we summarize the structures of POM-containing coordination polymers in which the combination of POMs and metal–organic polymers is through host–guest supramolecular interactions, such as weak coordination interactions, electrostatic interaction, and hydrogen bonding.

1. Introduction

POMs have numerous applications because of their unmatched diversity in composition, sizes and shapes [1–3]. While their various properties are garnering increasing attention, catalysis is still the most important area of application of POMs today [4]. POMs

* Corresponding author. Tel.: +86 591 83705794; fax: +86 591 83714946.
E-mail address: czlu@ms.fjirsm.ac.cn (C.-Z. Lu).

0010-8545/$ – see front matter © 2009 Elsevier B.V. All rights reserved.
doi:10.1016/j.ccr.2009.07.003

have been applied as acid and oxidation catalysts, including use in several large-scale industrial processes. However, their applications are limited due to their inherent drawbacks, including their low specific surface area, low stability under catalytic conditions, and their high solubility in aqueous solution. Many strategies to immobilize POMs on various porous solid supports have been studied in an effort improve their catalytic abilities [4a,5]. In addition to traditional inorganic and carbon-based porous materials, porous coordination polymers constructed from metal ions and doubly or multiply connecting ligands have recently appeared and become a new type of porous material. These materials are also referred as inorganic/organic hybrid polymers or porous metal–organic frameworks (MOF) [6]. Dispersing or immobilizing POMs by encapsulating them in the nanosized space of PCPs is a very promising approach to stabilize and optimize traditional POM materials as well as to convert homogeneous catalytic processes to heterogeneous catalytic processes by taking advantage of the high stability, high surface area, and low solubility of PCPs [7]. Furthermore, the dispersion of POMs in the pores of PCPs prevents the POMs from conglomerating and deactivating, which allows for the enhancement of their catalytic properties.

POM-containing coordination polymers have been of great interest since the beginning of this area [8]. By virtue of their diverse compositional range and significant structural versatility, polyoxometalates (POMs) are attractive inorganic building blocks [9]. They can coordinate to almost all metal atoms, including the transition metal and rare earth cations, leading to a family of compounds exhibiting widely diverse structures and physical–chemical properties [10]. As inorganic ligands, POMs range in size from sub nanoscale dimensions to the scale of proteins [11]. This diversity in size, coupled with their attractive electronic and molecular properties [12], has stimulated intensive investigation of supramolecular assemblies based on POMs in many important fields such as catalysis [4,13], photochemistry [14], nanotechnology [15], biology [16], materials science [17], medicine [18], magnetism [19], etc. Hundreds of POM-based coordination polymers have been synthesized, and many have been well summarized in reviews [9,20]. Herein, we will focus our emphasis on the PCPs/POM host–guest supramolecules in which the hosts are discrete metal–organic oligomers or metal–organic coordination polymers.

2. Synthesis

The rational synthesis of desired compounds by stepwise-predesigned routes has been used extensively in synthetic chemistry, for example in the total syntheses of natural products. However, the rational synthesis of PCPs/POM host–guest materials is still a great challenge because one or more of the reaction conditions, such as temperature, pH, stoichiometry, reaction time, medium, and template identity, can have considerable influence upon the reaction outcome. In fact, most PCPs/POM host–guest compounds have been synthesized via self-assembly reactions that are mainly driven by the coordination chemistry of each component.

Under ambient conditions, reactions of the starting building blocks for PCPs/POM supramolecules often produce amorphous precipitates instead of crystalline species. Because X-ray crystallography is the primary characterization technique in this area, suitable crystals are requisite for study. Hydrothermal reactions that have been well established in the preparation of traditional inorganic porous materials have been adapted to the preparation of crystals of POM-containing PCPs that would be difficult to obtain under ambient conditions [21]. Therefore, self-assembly of PCPs/POM supramolecules is usually performed under hydrothermal conditions.

3. PCPs/POM host–guest supramolecules

The structures of the PCPs/POM host–guest compounds are mainly composed of PCPs cations and POM anions. The POM anions may play various roles in these host–guest structures: (1) as templates to create the porous structures of PCPs; (2) as charge-compensating counterions; and (3) as ligands bound to the metal sites of PCPs via coordination bonds.

The self-assembly of coordination polymers is driven by the geometrical requirements of the ligands and the coordination preferences of the metal. Templates also play very important roles in the structures of PCPs. Without guest or template molecules to fill in the pores of the metal–organic coordination polymer, mutual interpenetration of the polymeric framework often occurs, and no porous structure forms [22]. By using POMs as templates, POM anions often fill some of the pores of the metal–organic polymer and prevent the cationic polymer from self-interpenetrating. This template effect is possibly the reason that self-interpenetration of POM-based coordination frameworks is not common.

In addition to being charge-compensating anions, POMs can be used to change the surface area of the PCPs. For example, Keggin anions $XM_{12}O_{40}^{n-}$ (M = Mo, W, . . ., X = P^{5+}, Si^{4+}, B^{3+}. . .), have comparable sizes while their negative charges can be made different by varying the heteroatoms. Therefore, the number of POM anions and the number of unoccupied pores in a PCP can be adjusted when different Keggin anions are used as counterions [23].

The oxygen atoms on the surface of POM molecules are unsaturated. They are still reactive enough to act as electron donors for various metal cations. In many cases, rather strong coordination interactions are generated, leading to direct coordination bonding between the cationic metal–organic component and the POM anions. However, the outer oxo groups of POMs are passivated by highly inward polarization, especially for heteropolyanions, with the result that the coordination bonds of POMs are often very weak. For example, the Cu–O distances between Cu ions and the POM anions in PCPs occur in a wide range of 2.10–2.90 Å, while the typical coordination bonding distance of a Cu–O bond is about 2.00 Å. Without question, the compounds with Cu–O bonds comparable to a typical Cu–O coordination distance are Class II supramolecules. Compounds with long coordination bonds (i.e., Cu–O > 2.50 Å), are reasonably categorized as Class I host–guest supramolecules. Therefore, the authors assert that, if the M-POM bonding distance in a POM PCP is 25% greater than the typical M–O bonding distance, the PCP should be classified as a Class I host–guest supramolecule.

Various organic heterocyclic nitrogen-containing compounds, including pyridine, pyrazine, phenanthroline, triazole, and imidazole, have been used as ligands in the construction of POM-based coordination polymers [9]. In this review, the linker is used as the basis for organization. The compounds reviewed are summarized in Table 1.

3.1. PCPs/POM host–guest supramolecules constructed from pyridyl ligands

3.1.1. Discrete metal-pyridyl clusters

The self-assembly of discrete 2 and 3D supramolecular complexes has been investigated extensively since the early 1990s [55]. Various molecular polygons have been synthesized from the combination of metal units and linear rigid 4,4′-bpy, and molecular recognition by the polygons is of interest in host–guest chemistry [56]. In 2007, Mizuno and coworkers synthesized a pair of Pd-based molecular triangles and squares that are in dynamic equilibrium in solution [25]. Reactions of the polygons with POMs form a series of molecular squares (**2**–**6**) with POMs as counteranions. Structural analysis indicates that the molecular square encapsulates $[W_6O_{19}]^{2-}$ and $[W_{10}O_{32}]^{4-}$ in compounds **2**–**4** but does not

Table 1
Selected structural information for host–guest porous coordination polymers formed from POM anions and metal–organic coordination polymers[a].

Compound	Metal–ligand framework	Metal coordination geometry	Structural description	Figure	Ref.
A. Bipyridine as linkers					
$[Ni_2(4,4'\text{-Hbpy})_4(4,4'\text{-bpy})(H_2O)_6](SiW_{12}O_{40})_2\cdot 16H_2O$ (**1**)	Dinickel compound	Octahedral $[NiN_3O_3]$	Discrete Ni units linked by POM via hydrogen bonds to form 1D chains		[24]
$\{[(en^*)Pd(4,4'\text{-bpy})]_4[\cdot W_6O_{19}]\}[W_6O_{19}]_3$ (**2**)	Molecular square	Square $[PdN_4]$	Molecular square with encapsulated POM	Fig. 1	[25]
$\{[(en^*)Pd(4,4'\text{-bpy})]_4[\cdot W_6O_{19}]\}(NO_3)_6$ (**3**)	As **2**	As **2**	As **2**		[25]
$\{[(en^*)Pd(4,4'\text{-bpy})]_4[\cdot W_{10}O_{32}]\}[W_{10}O_{32}]$ (**4**)	As **2**	As **2**	As **2**	Fig. 1	[25]
$[(en^*)Pd(4,4'\text{-bpy})]_4[W_{10}O_{32}]_2$ (**5**)	As **2**	As **2**	POM located outside of molecular square	Fig. 1	[25]
$[(en^*)Pd(4,4'\text{-bpy})]_4[\alpha\text{-}SiW_{12}O_{40}]_2$ (**6**)	As **2**	As **2**	As **5**	Fig. 1	[25]
$[\{Cu(4,4'\text{-bpy})\}_4(\delta\text{-}Mo_8O_{26})]$ (**7**)	1D	Diagonal $[CuN_2]$	POM encapsulated in a matrix of mutually perpendicular linear $[Cu(4,4'\text{-bpy})]^+$ chains with weak Cu···O interactions		[26]
$[\{Cu(4,4'\text{-bpy})\}_4Mo_{15}O_{47}]\cdot 8H_2O$ (**8**)	1D	Diagonal $[CuN_2]$	Layered structure of 1D POM chains and 1D linear $[Cu(4,4'\text{-bpy})]^+$ chains		[26]
$(H_3O)[Cu(4,4'\text{-bpy})]_3[\beta\text{-}Mo_8O_{26}]$ (**9**)	1D	Diagonal $[CuN_2]$	1D $[Cu(4,4'\text{-bpy})]^+$ chains linked to form 2D network by POM with weak Cu···O interactions		[27]
$K_3[Cu(I)(4,4'\text{-bpy})]_3[XW_{11}Cu(II)O_{39}]\cdot 11H_2O$ (X = Si, (**10**); X = Ge, (**11**))	1D	Diagonal $[CuN_2]$	2D POM layers between layers of 1D $[Cu(4,4'\text{-bpy})]^+$ chains		[28]
$[Cu(4,4'\text{-bpy})]\{[Cu(4,4'\text{-bpy})]_2[W_6O_{19}]\}\cdot 4H_2O$ (**12**)	1D	Diagonal $[CuN_2]$	Each POM interacts with four $[Cu(4,4'\text{-bpy})]^+$ through weak Cu···O interactions into 2D sheets	Fig. 2	[29]
$[Cu(bpe)]\{[Cu(bpe)]_2[GeMo_{12}O_{40}(VO)_2]\}$ (**13**)	1D	Diagonal $[CuN_2]$	1D $[Cu(bpe)]^+$ chains linked to form ladder-like double chains by POM through weak Cu···O interactions		[29]
$[Cu_3Cl(4,4'\text{-bpy}_3]_2[\alpha\text{-}SiW_{12}O_{40}]\cdot 4H_2O$ (**14**)	1D	T-shaped $[CuN_2Cl]$	1D linear $[Cu_3Cl(4,4'\text{-bpy})_3]^{2+}$ chains linked to form 2D network by POM with weak Cu···O interactions	Fig. 3	[30]
$\{Cu^{II}_4Cl(2,2'\text{-bipy})_4(4,4'\text{-bipy})_3(4,4'\text{-Hbipy})_2[PMo_{12}O_{40}]\}\ [PMo_{12}O_{40}]_2\cdot 2H_2O$ (**15**)	1D wave-like	$[CuN_4]$ $[CuN_4Cl]$	Wave-like chains linked into 2D sheets by POM through weak Cu···O interactions		[31]
$[Ni(4,4'\text{-Hbpy})_2(4,4'\text{-bpy})(H_2O)_2](SiW_{12}O_{40})\cdot 6H_2O$ (**16**)	1D	Octahedral $[NiN_4O_2]$	1D Ni chains linked by POM via hydrogen bonds to form 2D network	Fig. 4	[32]
$\{[Cu(4,4'\text{-bpy})_{1.75}]_4(SiW_{12}O_{40})(H_2O)_3\}_n$ (**17**)	1D with hexagonal motif	Trigonal $[CuN_3]$	POM encapsulated in the hexagonal voids of a pseudo-6^3-2D network from interlocking of 1D $[CuN_3]$ chains.	Fig. 5	[23]
$[Cu(4,4'\text{-bpy})(4,4'\text{-Hbpy})_{0.5}]_2[PW_{12}O_{40}]$ (**18**)	1D	Y-shaped $[CuN_3]$ and diagonal $[CuN_2]$	POM encapsulated in the pseudo-rectangular voids of a network from interlocking of 1D metal-organic chains.		[33]
$\{[(en)Pd(4,4'\text{-bpy})]_2[\alpha\text{-}SiW_{12}O_{40}]\}$ (**19**)	1D zigzag	Square $[PdN_4]$	Layered structure of 1D chains pillared by discrete POMs.	Fig.6	[34]
$\{[Ni(dpdo)_2(CH_3CN)(H_2O)_2]_2[SiW_{12}O_{40}](H_2O)_2\}_n$ (**20**)	1D	Octahedral $[MN_4O_2]$	POM anions between 2D layers of 1D chains interlocked through hydrogen bonds into pillared structure		[35]
$\{[M(dpdo)_4(H_2O)_3](H_3O)(SiMo_{12}O_{40})(dpdo)_{0.5}(CH_3CN)_{0.5}(H_2O)_3\}_n$ (M = Gd, (**21**); M = Ho, (**22**))	1D	$[MO_8]$	Shoulder-to-shoulder POMs encapsulated in rectangular voids of a 2D network of 1D chains interlocked by hydrogen bonds		[35]
$\{[Cu_2(4,4'\text{-bpy})_4(H_2O)_4](SiW_{12}O_{40})(H_2O)_{18}\}_n$ (**23**)	2D	Octahedral $[CuN_4O_2]$	Cationic square-grid network pillared by POM into layered structure	Fig. 7	[23]
$(4,4'\text{-bpy})[Zn(4,4'\text{-bpy})_2(H_2O)_2]_2[(ZnO_6)(As_3O_3)_2Mo_6O_{18}]\cdot 7H_2O$ (**24**)	2D	Octahedral $[ZnN_4O_2]$	As **23**		[36]
$\{Mn(2,2'\text{-bpy})(py)(H_2O)_2\}\{Mo_{12}O_{34}(bpy)_{12}\}][PMo_{12}O_{40}]_2\cdot 2H_2O$ (**25**)	2D	Octahedral $[MoO_4N_2]$ $[MnN_3O_3]$	Shoulder-to-shoulder POMs encapsulated in the pores of 2D networks	Fig. 8	[37]
$[Cu_3(4,4'\text{-bpy})_5(MeCN)_2]PW_{12}O_{40}\cdot 2C_6H_5CN$ (**26**)	3D	Tetrahedral $[CuN_4]$	POM resides in the pentagonal cavities of a 3D cationic polymer	Fig. 9	[38]
$[M_2(4,4'\text{-bpy})_3(H_2O)_2(ox)][P_2W_{18}O_{62}]_2(H_2\text{-bpy})\cdot nH_2O$ (M = Co(II), (**27**); M = Ni(II), (**28**))	3D	Octahedral $[MN_3O_3]$	3D non-interwoven framework with encapsulated POM anions	Fig. 10	[39]
$[Cu_2(H_2O)_2(bpp)_2Cl][PMo_{12}O_{40}]\sim 20H_2O$ (**29**)	3D	Octahedral $[CuClN_4O]$	3D non-interwoven framework with encapsulated POM	Fig. 11	[40]
$[Cu^{I}_3Cl(4,4'\text{-bpy})_4][Cu^{II}(1,10\text{-phen})_2Mo_8O_{26}]$(**30**)	3D	$[CuN_3Cl]$ $[CuN_2Cl]$ $[CuN_4O_2]$	3D $[Cu^{I}_3Cl(4,4'\text{-bpy})_4]$ framework with hexagonal channels in which $[Cu^{II}(1,10\text{-phen})_2Mo_8O_{26}]$ chains are located		[27]
$[\{Fe(tpypor)\}_3Fe(Mo_6O_{19})_2]\cdot xH_2O$ (**31**)	3D	Octahedral $[FeN_6]$	POMs encapsulated within 3D cationic polymer with cubic $\{Fe_8(tpypor)_6\}^{8+}$ building blocks		[41]
$\{[M_4(dpdo)_{12}][H(H_2O)_{27}(CH_3CN)_{12}][PW_{12}O_{40}]_3\}_n$ (M = Co, (**32**); M = Ni, (**33**))	3D	Octahedral $[MN_6]$	POMs and gigantic water clusters encapsulated within 3D non-interwoven framework	Fig. 12	[35]
$\{[Ln(H_2O)_4(pdc)]_4\}[XMo_{12}O_{40}]\cdot 2H_2O$ (Ln = La, Ce, and Nd; X = Si for **34**-**36** and Ge for **37**-**39**.)	3D	$[MNO_8]$	3D lanthanide framework with encapsulated POM anions		[42]
B. Pyrazine as linkers					
$[Ag_3(pz)_3(PW_{12}O_{40})]\cdot 0.5H_2O$ (**40**)	1D	Trigonal $[AgN_2]$	POM anions encapsulated in the matrix of 1D $[Agpz]^+$ chains		[23]

Table 1 (*Continued*)

Compound	Metal–ligand framework	Metal coordination geometry	Structural description	Figure	Ref.
$Cu_4(2\text{-pzc})_4(H_2O)_8(Mo_8O_{26})\cdot 2H_2O$ (**41**)	1D zigzag	Diagonal $[CuN_2]$	Each POM is surrounded by 5 chains		[43]
$\{[Cu(pz)(H_2O)_4]_2(H_3O)_2[V_{10}O_{28}]\cdot 13.5H_2O\}_n$ (**42**)	1D	Octahedral $[CuN_2O_4]$	Layered structure with alternating layers of 1D chains and POM		[44]
$\{[Ni(pz)(H_2O)_4]_2(H_3O)_2[V_{10}O_{28}]\cdot 9.5H_2O\}_n$ (**43**)	1D	Octahedral $[CuN_2O_4]$	As **42**		[44]
$Cu_3(2\text{-pzc})_4(H_2O)_2(V_{10}O_{28}H_4)\cdot 6.5H_2O$ (**44**)	2D rectangle grid-like	Square $[CuN_2O_2]$ Octahedral $[CuN_2O_4]$	POMs encapsulated within the rectangles of a 2D network		[43]
$\{[Cu(pz)_{1.5}]_4(SiW_{12}O_{40})\cdot 2H_2O\}_n$ (pz = pyrazine) (**45**)	2D octagonal and square units	Trigonal $[CuN_3]$	POM encapsulated in the octagons of unique 2D 4^18^2 network	Fig. 13	[23]
$\{[Cu(2,3\text{-}Me_2pz)_{1.5}]_4(SiW_{12}O_{40})\}_n$ (**46**)	As **45**	Trigonal $[CuN_3]$	As **45**		[23]
$\{[Cu(2,3\text{-}Me_2pz)(2,5\text{-}Me_2pz)_{0.5}]_4(SiW_{12}O_{40})(2,5\text{-}Me_2pz)\}_n$ (**47**)	2D hexagonal units	Trigonal $[CuN_3]$	The layers of 2D 6^3 networks pillared by POM into layered structure		[23]
$\{[Cu(2\text{-}Mepz)_{1.5}]_3(PMo_{12}O_{40})(H_2O)_{3.5}\}_n$ (**48**)	2D hexagonal units	Trigonal $[CuN_3]$	As **47**		[23]
$\{[Ag(2,3\text{-}Me_2pz)_{1.5}]_4(SiW_{12}O_{40})\}_n$ (**49**)	2D hexagonal units Corrugated	Trigonal $[CuN_3]$	The layers of 2D corrugated 6^3 networks pillared by POM into layered structure	Fig. 14	[23]
C. Triazole as linkers					
$[Ag_4(dmtrz)_4][\beta\text{-}Mo_8O_{26}]$ (**50**)	Tetranuclear Ag cluster	Diagonal $[AgN_2]$	Each POM surrounded octahedrally by six Ag clusters		[45]
$[Ag_6(3atrz)_6][PMo_{12}O_{40}]_2\cdot H_2O$ (**51**)	A double calix[3]arene-shaped hexamer	Diagonal $[AgN_2]$	POM anions encapsulated between $[Ag_6(3atrz)_6]$ hexamers	Fig. 15	[45]
$[Cu^I_4(Hfcz)_4(SiMo_{12}O_{40})]$ (**52**)	Molecular square	Diagonal $[CuN_2]$	Molecular square linked by POM via weak Cu···O interactions into 2D network	Fig. 16	[46]
$[Ag_2(trz)_2]_2[\gamma\text{-}Mo_8O_{26}]$ (**53**)	1D zigzag chain	Diagonal $[AgN_2]$	Layered structure with mutually perpendicular 1D $[\gamma\text{-}Mo_8O_{26}]^{4-}$ chains and 1D zigzag $[Ag(trz)]^+$ chains	Fig. 17	[45]
$[Ag_4(4atrz)_2Cl][Ag(Mo_8O_{26})]$ (**54**)	1D looped chain	$[AgN_2]$ $[AgNCl]$	Mutually perpendicular 1D $[Ag(Mo_8O_{26})]^{3-}$ chains and 1D zigzag $[Ag(trz)]^+$ chains	Fig. 18	[45]
$[Ag_2(3atrz)_2]_2[HPMo^{VI}{}_{10}Mo^{V}{}_2O_{40}]$ (**55**)	1D helix	Diagonal $[AgN_2]$	Hydrogen bonding between helical chains and POMs	Fig. 19	[45]
$[Ag_2(dmtrz)_2]_2[HPMo^{VI}{}_{10}Mo^{V}{}_2O_{40}]$ (**56**)	Same as **55**	Diagonal $[AgN_2]$	Same as **55**		[45]
$(Et_3NH)_2[Cu^I_2(Hfcz)_2(SiW_{12}O_{40})]\cdot 2H_2O$ (**57**)	1D zigzag	Diagonal $[CuN_2]$	1D copper chains linked by POM via weak Cu···O interactions	Fig. 20	[46]
$(Et_3NH)_2[Cu^I_2(Hfcz)_2(SiW_{12}O_{40})]\cdot H_2O$ (**58**)	1D zigzag	Diagonal $[CuN_2]$	As **57**	Fig. 21	[46]
$[Cu_4(H_2O)_4(bte)_2(HPMo^{VI}{}_{10}Mo^{V}{}_2O_{40})]\cdot 2H_2O$ (**59**)	1D	Tetrahedral $[CuN_2O_2]$ Diagonal $[CuN_2]$	1D $[Cu_2(H_2O)_2(bte)]^{2+}$ chains linked by POMs via weak Cu···O interactions to form ladder-like chains and then stair-like 2D network		[47]
$[Cd_2(Hfcz)_6(H_2O)_2](SiMo_{12}O_{40})\cdot H_2O$ (**61**)	1D hinge	Octahedral $[CdN_6]$ $[CdN_4O_2]$	POMs located between layers of the 1D chains		[46]
$[Cu(btb)][Cu_2(btb)_2(PMo_{12}O_{40})]$ (**62**)	1D	Diagonal $[CuN_2]$	Part of 1D $[Cu(btb)]^+$ chains linked by POMs via weak Cu···O interactions form 2D sheets; other 1D chains and the 2D sheets arrange alternately into a layered structure	Fig. 22	[47]
$[Cu_4(btb)_2(SiMo_{12}O_{40})]\cdot 2H_2O$ (**63**)	1D channel-like	Diagonal $[CuN_2]$	1D $[Cu_4(btb)_2]^{4+}$ chains linked by POMs via weak Cu···O interactions to form 3D framework	Fig. 23	[48]
$[\alpha\text{-}Cu_{12}(trz)_8][PMo_{12}O_{40}]\cdot H_2O$ (**64**)	2D octagonal and square Cu-polygons units	Diagonal $[AgN_2]$	Layered structure with POMs encapsulated in Cu-octagons	Fig. 24	[49]
$[\beta\text{-}Cu_{12}(trz)_8][PMo_{12}O_{40}]\cdot 2H_2O$ (**65**)	2D triangular and nonagonal Cu-polygons	Diagonal $[AgN_2]$	Layered structure with POMs encapsulated in Cu-nonagons		[49]
$[Co_2(Hfcz)_2(SiW_{12}O_{40})](H_3fcz)_2(SiW_{12}O_{40})\cdot 10H_2O$ (**66**)	2D double-layered	Octahedral $[CoN_4O_2]$	2D layers of $[Co(Hfcz)_2(H_2O)]_n$ linked by POMs covalently to form double-layered 2D networks which are in turn pillared by other non-coordinated POM anions into a layered structure	Fig. 25	[50]
$[Cu^{II}(L)_2(H_2O)_2][Cu^I_2(L)_2]PMo_{12}O_{40}]$ (**67**) (L = 4,4′-bis(1,2,4-triazol-1-ylmethyl) biphenyl)	3D and 0D molecular square	Diagonal $[CuN_2]$ Octahedral $[CuN_4O_2]$	POM anions encapsulated in 3D [3] rotaxane framework of twofold interpenetrated adamantanoid cages with additional locking of molecular squares	Fig. 26	[51]
D. Imidazole as linkers					
$(bbi)_{1.5}[Cu(bbi)]_{4.5}[PW_{12}O_{40}]_{1.5}$ (**68**)	1D	Diagonal $[CuN_2]$	POMs encapsulated in the channels created by 5 1D chains with weak Cu···O interaction		[52]
$[Cu^I(bbi)]_2[Cu^I_2(bbi)_2(\delta\text{-}Mo_8O_{26})_{0.5}](\alpha\text{-}Mo_8O_{26})_{0.5}$ (**69**)	1D	Diagonal $[CuN_2]$	1D chains connected by POMs via weak Cu···O interaction to form a complex polythreaded structure	Fig. 27	[53]
$[Cu^I(bbi)][Cu^I(bbi)(\theta\text{-}Mo_8O_{26})_{0.5}]$ (**70**)	1D	Diagonal $[CuN_2]$	1D chains connected by POMs via weak Cu···O interaction to form double chains and then with additional 1D chains to form a polythreaded structure		[53]
$[H_2bbi][Cu^{II}(bbi)_2(\beta\text{-}Mo_8O_{26})]$ (**71**)	2D rectangle	Square $[CuN_4]$	2D $[Cu(bbi)_2]^{2+}$ sheets connected by POM anions into 3D framework via weak Cu···O interaction	Fig. 28	[54]

Table 1 (*Continued*)

Compound	Metal–ligand framework	Metal coordination geometry	Structural description	Figure	Ref.
$[Cu^{II}(bbi)_2(H_2O)(\beta\text{-}Mo_8O_{26})_{0.5}]$ (**72**)	2D rectangle	Square $[CuN_4]$	2D $[Cu(bbi)_2]^{2+}$ sheets connected by POM anions via weak Cu···O interaction into 3D framework, twofold penetration of the 3D framework		[54]
$[Cu^{II}(bbi)_2(\alpha\text{-}Mo_8O_{26})][Cu^{I}(bbi)]_2$ (**73**)	rectangular 2D sheets plus 1D chains	Square $[CuN_4]$ Diagonal $[CuN_2]$	2D $[Cu^{II}(bbi)_2]_n^{2n+}$ layers pillared by POMs via weak Cu···O interactions to form a 3D structure with channels of 1D chains inside	Fig. 29	[54]
$[Cu^{II}Cu^{I}(bbi)_3(\alpha\text{-}Mo_8O_{26})][Cu^{I}(bbi)]$ (**74**)	2D with large rings plus 1D chains	Square $[CuN_4]$ Diagonal $[CuN_2]$	2D $[Cu^{II}Cu^{I}(bbi)_3]_n^{3n+}$ layers pillared by POMs via weak Cu···O interaction to form a 3D structure with channels of 1D chains inside		[54]

[a] *Abbreviations*: 3atrz = 3-amino-1,2,4-triazole; 4atrz = 4-amino-1,2,4-triazole; bbi = 1,10-(1,4-butanediyl)bis(imidazole); bpe = bis(4-pyridyl)ethylene; bpp = 1,3-bis(4-pyridyl) propane; bpy = bipyridine; btb = 4-bis(1,2,4-triazol-1-y1)butane; bte = 1,2-bis(1,2,4-triazol-1-yl)ethane; dmtrz = 3,5-dimethyl-1,2,4-triazole; dpdo = 4,4′-bipyridine-*N*,*N*′-dioxide; en* = *N*,*N*,*N*′,*N*′-tetramethylethylenediamine; en = ethylenediamine; Hfcz = 2-(2,4-difluorophenyl)-1,3-di(1*H*-1,2,4-triazol-1-yl)propan-2-ol; H_2pdc = pyridine-2,6-dicarboxylate; H(2-pzc) = 2-pyrazine-carboxylic acid; 2,3-Me_2pz = 2,3-dimethylpyrazine; 2,5-Me_2pz = 2,5-dimethylpyrazine; 2-Mepz = 2-methylpyrazine; ox = oxalate; phen = phenanthroline; pz = pyrazine; trz = 1,2,4-triazole; tpypor = tetrapyridylporphyrin.

encapsulate the α-$SiW_{12}O_{40}^{4-}$ anion, which is bigger than those in **2**–**4**, as shown in Fig. 1. The size-selective encapsulation by the molecular square is interesting and could be used in the separation or purification of useful polyoxometalates.

3.1.2. One-dimensional metal-pyridyl polymers

One-dimensional metal-pyridyl chains are common in POM-based coordination polymers, as revealed in compounds **7**–**22**. The detailed structures of the 1D chains are affected by various factors, including the coordination preferences of the metals, the metal–ligand stoichiometry, the reaction conditions, the presence of coligands, and the template effect of counteranions. In compounds **7**–**14**, the Cu(I) metal sites are linked by the pyridyl ligands into linear $[Cu(4,4'\text{-bpy})]^+$ chains, which reflects the preference of d^{10} for diagonal coordination. Weak coordination interaction between the chains and the POM anions exists frequently in these compounds. For example, in compound **12**, each $[W_6O_{19}]^{2-}$ dianion acts as a tetradentate ligand through weak coordination bonding (Cu···O 2.633(9) and 2.696(9) Å) to bind four $[Cu(4,4'\text{-bpy})]_n^{n+}$ chains, resulting in a rare double bitrack Cu(4,4′-bpy) chain-modified Lindqvist polymeric compound (Fig. 2) [29].

The structure of compound **14** demonstrates the influence of coligands. In compound **14**, three $[Cu(4,4'\text{-bpy})]^+$ chains are linked through Cl^- anions into a rare Cu(I) polymeric $\{[Cu(4,4'\text{-bpy})]_3Cl\}^{2+}$ structure, as shown in Fig. 3 [30]. The trimeric chains are linked by POM anions through weak Cu···O interactions into a 2D layered network.

Compound **16** is an example that shows the influence of hydrogen bonding interactions on the formation of metal–organic polymer/POM host–guest structures [23]. The compound contains 1D chains of $[Ni(4,4'\text{-Hbpy})_2(4,4'\text{-bpy})(H_2O)_2]_n^{4n+}$ cationic polymers, which are composed of 1D linear [Ni (4,4′-bpy)] chains with two additional pendant monoprotonated 4,4′-Hbpy ligands coordinating each Ni(II) site. The 1D cationic chains are then linked into 2D supramolecular layers by POM anions through hydrogen bonding, as shown in Fig. 4.

The template effect of POM anions is illustrated in the structures of compounds **17**–**19**. These compounds contain particularly unusual 1D chains that have never been observed without the pres-

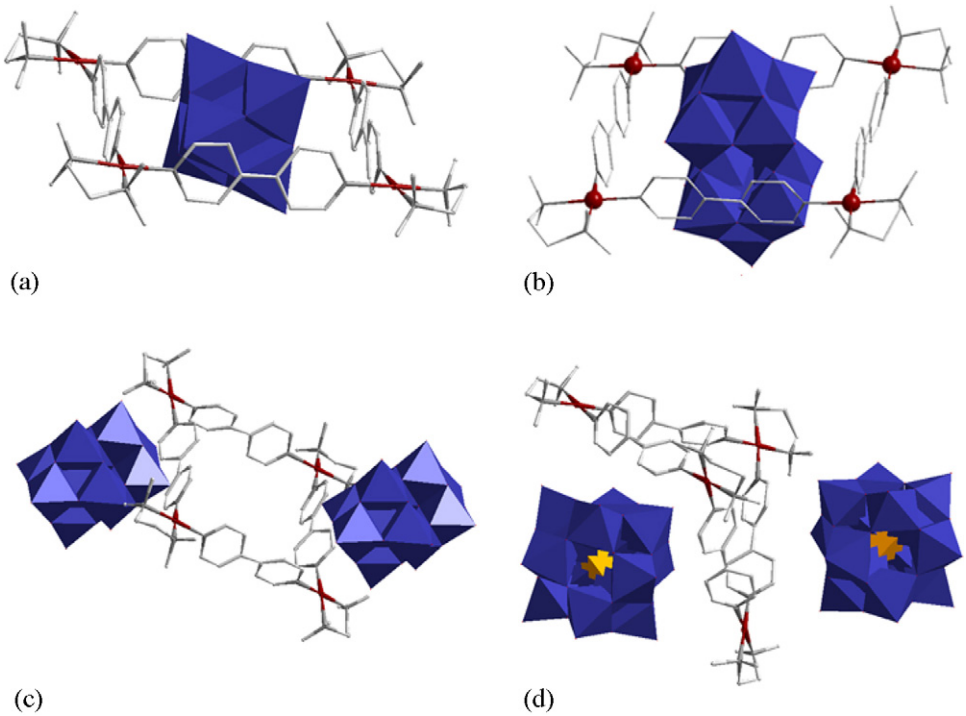

Fig. 1. Structures of compounds: side views of **2** (a) and **4** (b) showing the encapsulation of the polyanion in the molecular square; top views of **5** (c) and **6** (d).

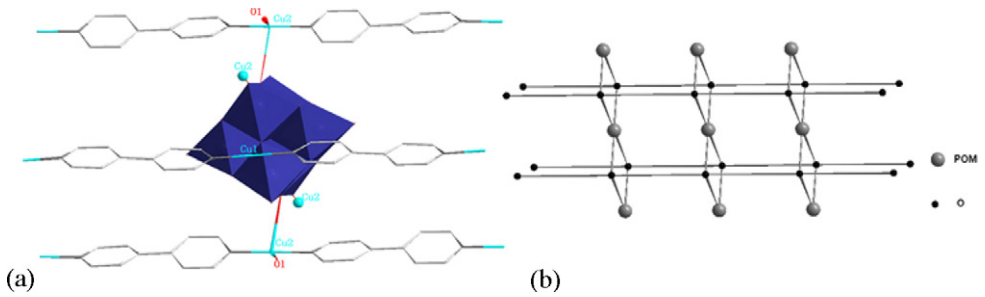

Fig. 2. Structures of **12** (a) building blocks. (b) Schematic view of the layer structure consisting of double bitrack Cu(4,4′-bpy) chain-modified POMs.

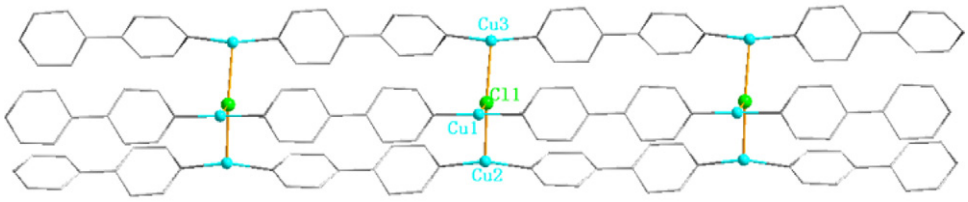

Fig. 3. A view of the trimeric Cu(I) cationic chain in **14**.

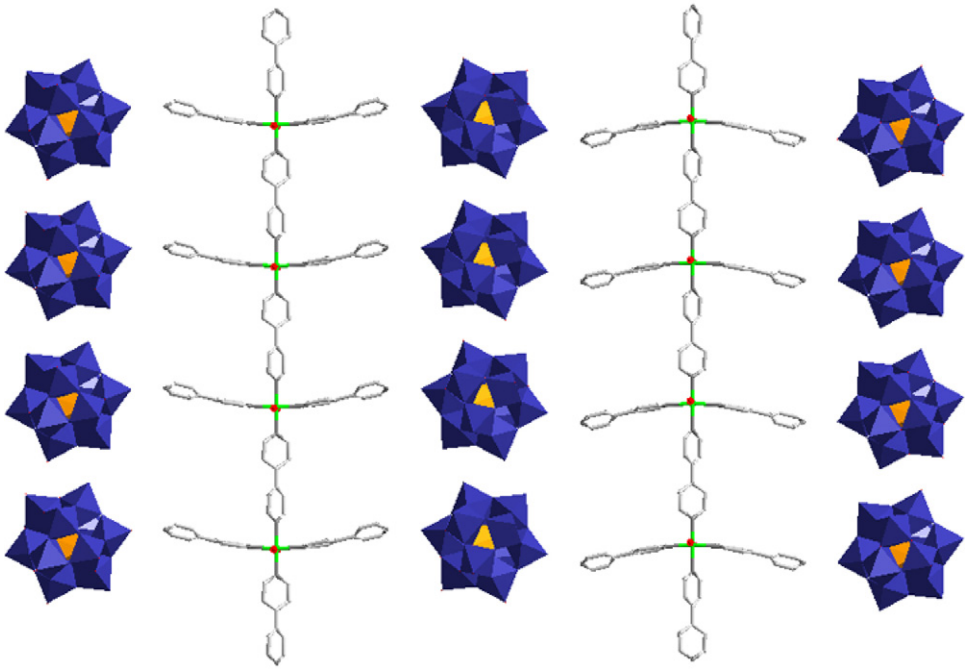

Fig. 4. A view of the 2D structure in compound **16**.

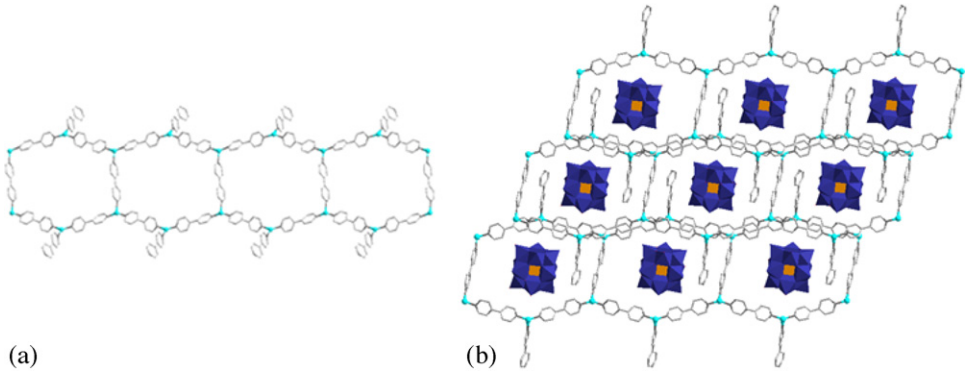

Fig. 5. Views of compound **17**: (a) showing the 1D chain with hexagonal units and (b) showing the $SiW_{12}O_{40}^{4-}$ anions encapsulated in the pseudo-6^3 2D network.

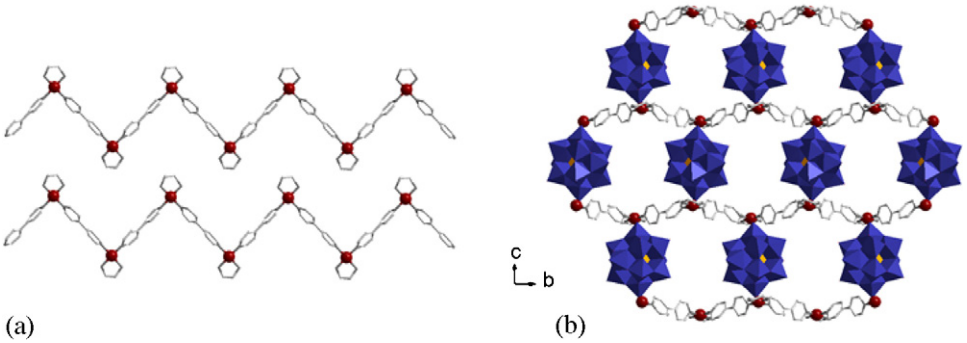

Fig. 6. A view of the cationic polymer (a) and layered structure (b) of compound **19**.

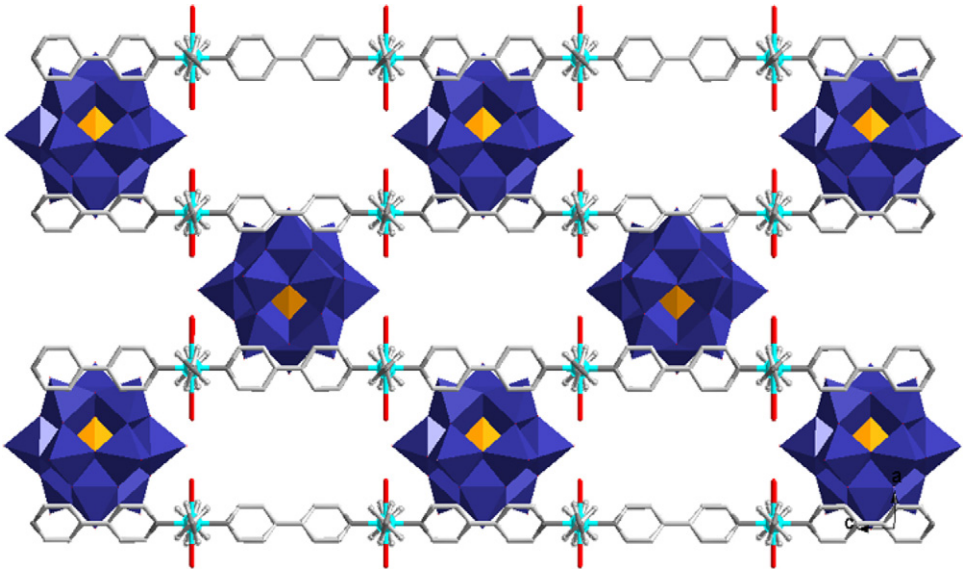

Fig. 7. A view of compound **23** showing the layered structure with $SiW_{12}O_{40}^{4-}$ as pillars.

ence of the POM anions. For example, compound **17** has a unique 1D chain with hexagonal units (Fig. 5) [23]. A survey of the CSD revealed that such a hexagonal void structure has not been found in copper(I or II)-4,4′-bpy complexes. Interlocking the adjacent chains generates a pseudo-6^3 2D network. The $SiW_{12}O_{40}^{4-}$ anions are encapsulated in the resulting hexagonal cavities.

The structure of compound **19** (as shown in Fig. 6) is composed of $SiW_{12}O_{40}^{4-}$ anions and infinite 1D zigzag $[(en)Pd(4,4'\text{-bpy})]_n^{2n+}$chains [34]. The formation of the 1D chains is very surprising because the combination of partially blocked $[(en)Pd]^{2+}$ metal building blocks, which were used as starting materials in the preparation of compounds **2**–**6**, with rigid linear 4,4′-bpy ligands in a 1:1 ratio under ambient conditions results preferentially in the formation of molecular polygons, such as $[(en^*)Pd(4,4'\text{-bpy})]_n(NO_3)_{2n}$ (n = 3, or 4).

3.1.3. Two-dimensional metal-pyridyl polymers

The structure of compound **23** is composed of 2D layers of $[Cu(4,4'\text{-bpy})_2(H_2O)_2]_n^{2n+}$, Keggin $SiW_{12}O_{40}^{4-}$ polyanions and water molecules [23]. The sheets are constructed from a square-grid motif and stacked in parallel fashion. The resulting 2D channels are occupied alternately by Keggin anions and cage-like $(H_2O)_{14}$ clusters. The $SiW_{12}O_{40}^{4-}$ anions locate between the 2D sheets rather than penetrate them, perhaps due to the size limits of the square units as in compound **6**, leading to a layer-pillared 3D structure as shown in Fig. 7. Compounds **24** and **25** have similar 3D layered structure s with POM polyanions as pillars.

Compound **25** is composed of $[PMo_{12}O_{40}]^{3-}$ anions and unusual 2D heteronuclear cationic sheets with very large pores (ca. 28.3 × 11.7 Å) [37]. The 2D sheet can be considered as being constructed from wave-like 1D chains of $[Mo_{12}O_{34}(bpy)_{12}]_n^{4n+}$ and $[Mn(bpy)(py)(H_2O)_2]$ joints. Adjacent 1D Mo chains are linked through the Mn units to produce a 2D network with 26-metal cyclic units. The pore of the cyclic unit is so large that two Keggin ions (ca. 10.4 × 10.4 Å) are encapsulated in a “shoulder by shoulder” mode as shown in Fig. 8. Furthermore, the neighboring 2D networks are stacked parallel to each other along the *c*-axis to generate a 3D supramolecular framework through extensive hydrogen bonds between bpy ligands and terminal oxygen atoms from adjacent molybdenum oxide layers.

3.1.4. Three-dimensional metal-pyridyl polymers

The structure of compound **26** has a unique 3D framework. The influence of the $PW_{12}O_{40}^{3-}$ polyanion as a non-coordinating anionic template in the construction of this structure is evident [38]. In this compound, the Cu(I) sites adopt $[CuN_4]$ tetrahedral coordination with bridging 4,4′-bpy ligands or a terminal CH_3CN ligand. Five Cu(I) centers, of which three are coordinated by three bridging 4,4′-bpy ligands and one terminal CH_3CN molecule while the other two are coordinated by four bridging 4,4′-bpy ligands, are assembled around a POM anion by shared bridging 4,4′-bpy ligands to form an interesting pentagonal unit (Fig. 9). The pentagonal units are linked further through 4,4′-bpy into a 3D framework.

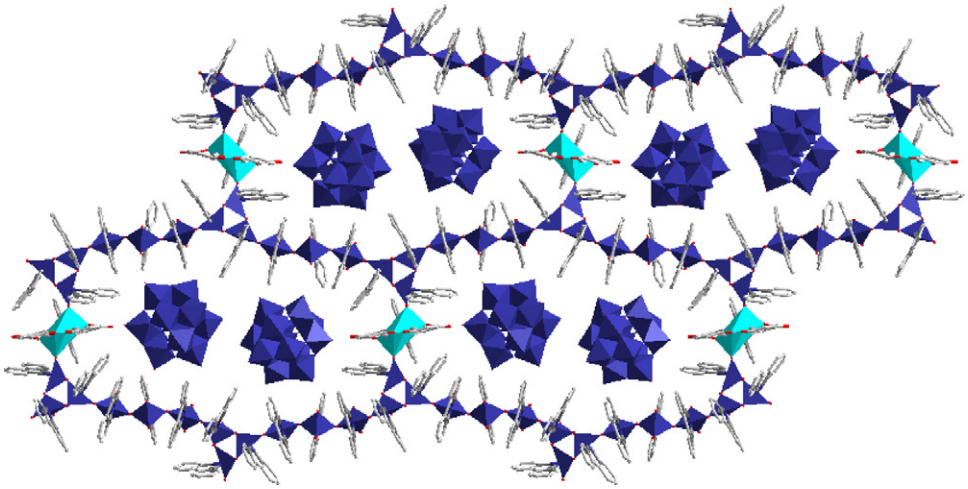

Fig. 8. Polyhedral representation of **25**: $\{MoO_4N_2\}$ octahedra, blue; $\{MnO_3N_3\}$ octahedra, azure; Keggin polyanions, blue.

The influence of metal coordination preference and coligand is evident in the structures of **27** and **28**, which are isomorphous [39]. In these compounds, each M(II) center is coordinated in a distorted octahedral geometry by two oxygen atoms from an oxalate (ox) ligand, one terminal water molecule and three nitrogen atoms from 4,4′-bpy bridging ligands. Two identical M(II) units are connected by sharing a μ_4-oxalate ligand to form binuclear secondary building units (SBUs) which act as pseudo-octahedral six-connected nodes (Fig. 10). Each SBU is connected to six identical SBUs through 4,4′-bpy bridges into a 3D porous coordination framework. The resulting square channels are occupied alternately by Dawson $P_2W_{18}O_{62}^{6-}$ anions and interstitial molecules, including H_2O molecules and protonated H_2-4,4′-bpy.

Compound **29** is a 3D POM-based coordination polymer containing a tethered 4-pyridyl ligand, 1,3-bis(4-pyridyl) propane (bpp) [40]. The dramatic influence of introducing a flexible spacer between the nitrogen donor groups is shown in this instance. In this compound, the Cu(II) atoms are coordinated in a distorted

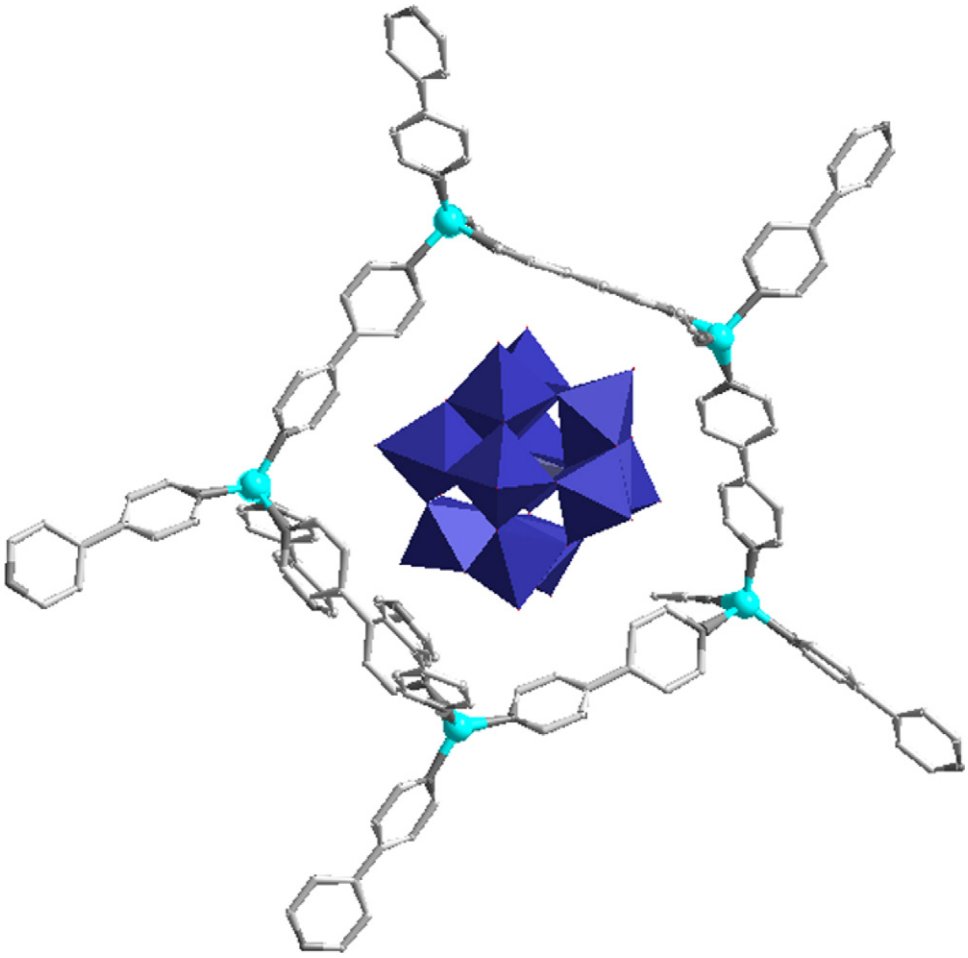

Fig. 9. The framework (host) and the POM (guest) in compound **26**.

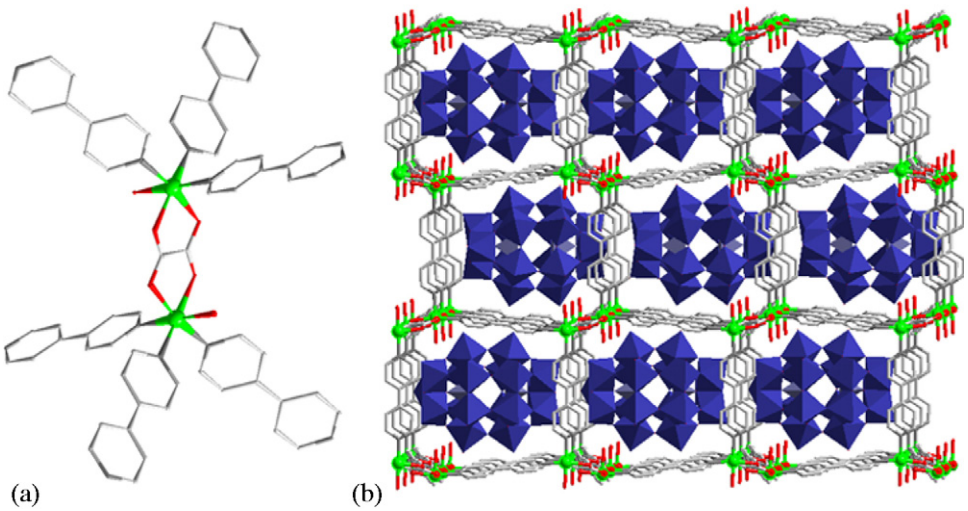

Fig. 10. Structural illustrations of compounds **27** and **28**. (a) A view of the dinuclear SBU. (b). A view of the 3D host framework with the entrained $P_2W_{18}O_{62}^{6-}$ polyanions (polyhedra).

octahedral geometry by four N atoms from four bridging bpp ligands, one water molecule and one bridging Cl anion. Two identical Cu(II) units are linked by sharing a bridging Cl^- anion to form a binuclear SBU, which acts as an eight-connected [Cu_2] building unit. Each dinuclear unit is further linked to eight nearest-neighbors through eight bpp ligands into a bcc-type 3D porous coordination polymer (Fig. 11). The 3D framework features various nanosized channels. Two kinds of large channels can be observed along the [1 1 0] direction with dimension of 13.8 Å × 14.6 Å and 13.9 Å × 12.5 Å, respectively, which are occupied by the Keggin-type ions (ca. 10.4 Å × 10.4 Å).

As shown in Table 1, several 4,4′-bpy-containing 3D coordination polymer/POM host–guest compounds have been reported so far. However, all of the hosts in these compounds are heteroleptic.

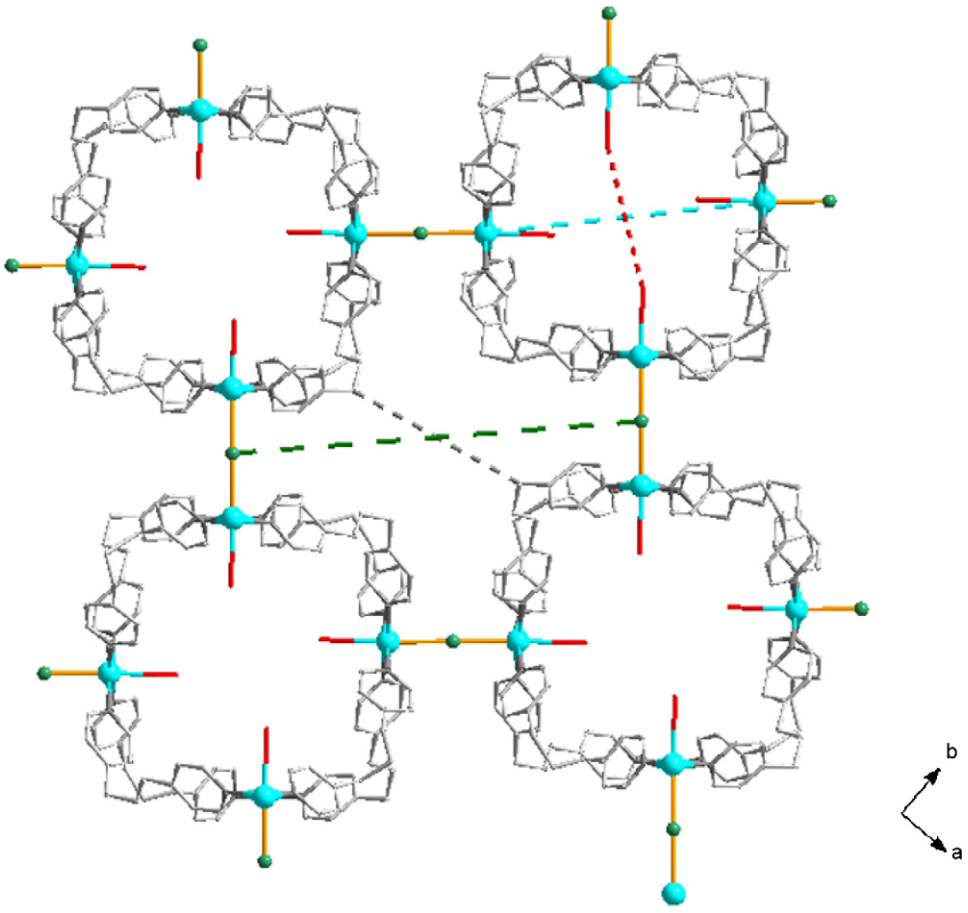

Fig. 11. View of the structure of **29** along the [1 1 0] direction.

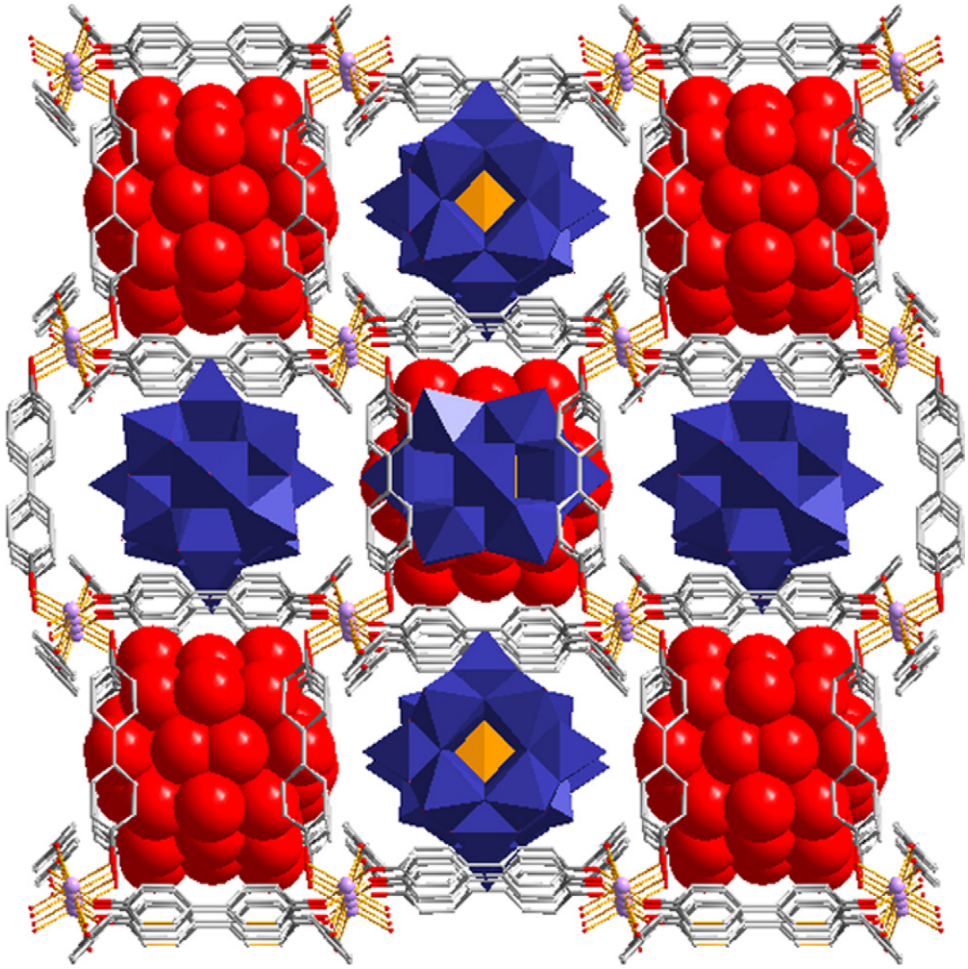

Fig. 12. Packing diagram of compounds **32** and **33** along the *c*-axis showing the cubic molecular boxes, which serve as hosts to contain the POMs (blue polyhedra) and the protonated water cluster $H^+(H_2O)_{27}$ (red space-filling).

No homoleptic 4,4′-bpy 3D hosts have been synthesized thus far. A possible reason is the size limitation of the cavities in such 3D coordination polymers. Recently, by using the 4′-bpy derivative ligands 4,4′-bipyridine-*N*,*N*′-dioxide and tpypor, in which the distances between donor groups are lengthened, the 3D homoleptic coordination polymer/POM host–guest compounds **31**–**33** were successfully assembled. Compound $[\{Fe(tpypor)\}_3Fe(Mo_6O_{19})_2]\cdot xH_2O$ (**31**) contains a three-dimensional $[\{Fe(tpypor)\}_3Fe]_n^{4n+}$ cationic framework and isolated $\{Mo_6O_{19}\}^{2-}$ polyoxo anions [41]. The resulting cubic cavities are alternately occupied by $\{Mo_6O_{19}\}^{2-}$ clusters and disordered water molecules.

In compounds **32** and **33**, each M(II) center is coordinated in an essentially ideal octahedral geometry to six dpdo bridging ligands [35]. The sharing of the bridging dpdo ligands of the metal atoms creates a 3D non-interwoven porous coordination framework. The resulting channels are occupied by either the $PW_{12}O_{40}^{3-}$ anions or CH_3CN-stablized water clusters $H^+(H_2O)_{27}$ (Fig. 12). The structure of the water clusters in these compounds is an interesting composition of a 26 water $(H_2O)_{26}$ shell and a monowater center, which act as "host" and "guest", respectively.

3.2. PCPs/POM host–guest supramolecules constructed from pyrazine

The coordination preference of pyrazine is similar to that of 4,4′-bpy. As shown in Table 1, several 1D and 2D POM-based coordination polymers have been synthesized. However, the short distance between the donor groups causes difficulty in forming 3D compounds with POM anions as guests. No 3D pyrazine coordination polymer/POM host–guest compounds have been reported so far.

Compounds **45**–**49** are composed of 2D coordination polymers with pyrazine and its derivatives as bridging unit [23]. Their structures show again the structural flexibility of coordination polymers and the influence of the steric groups in the ligands. Compound **45** is composed of a 2D $[Cu(pz)_{1.5}]_n^{n+}$ framework and $SiW_{12}O_{40}^{4-}$ anions. In this compound, each Cu(I) atom is coordinated trigonally to three pz bridging ligands [23]. The 2D framework can be viewed as being constructed from square tetranuclear building blocks that are composed of four Cu(I) centers and four pz bridging ligands. Each tetranuclear building block is linked to four others of the same kind by the pz ligands. This arrangement leads to the formation of a 2D layer which can be visualized more simply as a unique $4^1 8^2$ network with each Cu(I) center lying next to one square void and two octagonal voids. The octagonal void is so large that the $SiW_{12}O_{40}^{4-}$ anion can be encapsulated inside it. The replacement of pz in **45** by 2,3-Me_2pz allowed the formation of compound **46** (Fig. 13), the structure of which is similar to that of complex **45** [23].

Complexes **47**, **48**, and **49** have common structural features [23]. In these compounds, linkage of the trigonal $[MN_3]$ units leads simply to the generation of 2D 6^3 networks with hexanuclear motifs. The 2D sheets in compounds **47** and **48** are essentially planar, but compound **49** has a corrugated structure (Fig. 14). In contrast to the octagonal voids in **45** and **46**, the hexagonal voids are not

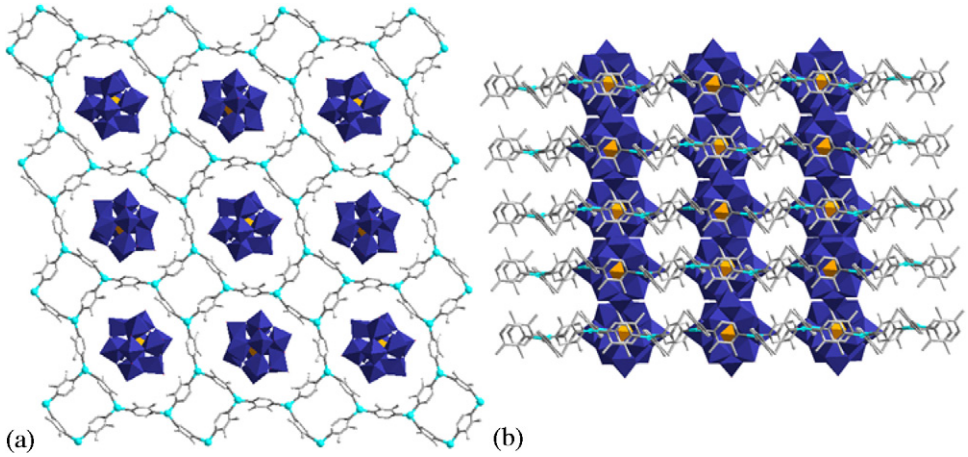

Fig. 13. Views of structure **46** (a) 2D structure of the $[Cu(pz)_{1.5}]_n^{n+}$ polymeric cation with encapsulated polyanions. (b) Crystal packing showing that the polyanions penetrate the 2D polymeric cation.

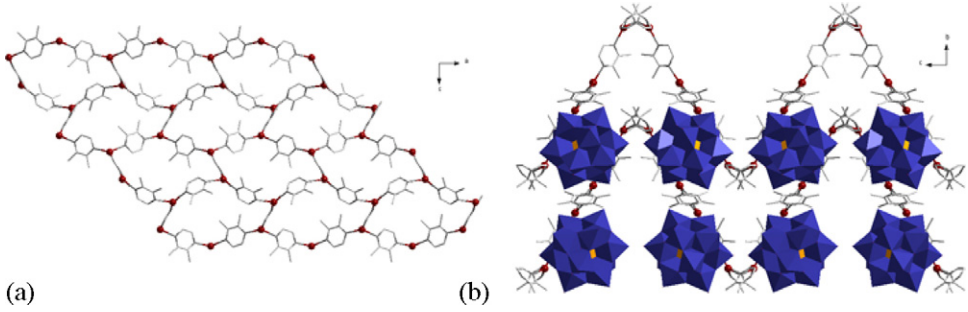

Fig. 14. Views of structure **49**. (a) Structure of 2D sheet. (b) Crystal packing.

large enough to accommodate fully a Keggin anion. In these complexes, Keggin anions are located between the 2D layers to form 3D layer-pillared structures, as in compound **23**. Owing to the charge difference between $PMo_{12}O_{40}^{3-}$ and $SiW_{12}O_{40}^{4-}$, the $PMo_{12}O_{40}^{3-}$ anions occupy two-thirds of the hexagonal voids in **48** instead of half of the voids in **47** and **49**. These examples demonstrate that the number of voids in coordination polymers can be manipulated with the corresponding charge of the POMs.

3.3. PCPs/POM host–guest supramolecules constructed from triazole ligands

Recently, 1,2,4-triazole and its derivatives have gained increasing attention in the coordination chemistry of transition metals, not only because of their numerous coordination possibilities, but also because of their wide-ranging potential as pharmaceuticals, agricultural chemicals, and photographic materials. By virtue of their versatile coordination abilities, many simple 1,2,4-triazole compounds and their tethered derivatives have been used in the construction of POM-based coordination polymers.

3.3.1. Discrete metal-triazole clusters

Complex **51** is composed of discrete $[Ag_6(3atrz)_6]^{6+}$ cationic hexamers and non-coordinated $[PMo_{12}O_{40}]^{3-}$ anions [45]. Each silver atom is diagonally coordinated by two 3atrz bridging ligands, and the 3atrz ligands serve as bridging ligands in a common N1, N2 mode to link silver atoms. This arrangement leads to the formation of a double calix[3]arene-shaped hexamer with two bowls, each containing a polyanion, opening in opposite directions and sharing a common bottom (Fig. 15). In packing in the crystalline state,

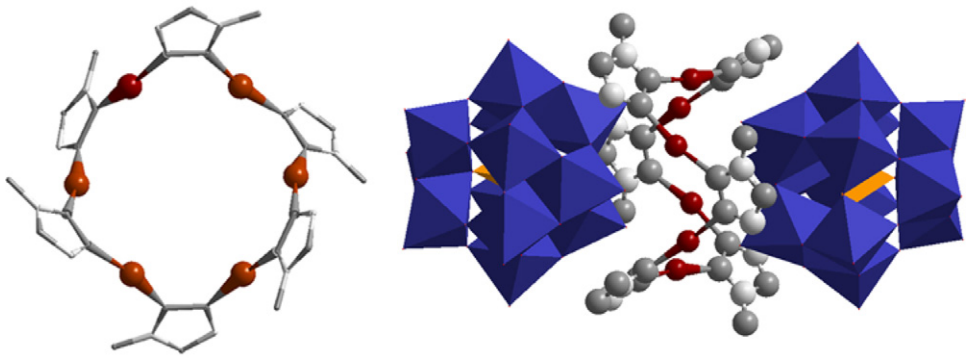

Fig. 15. (a) The structure of the hexanuclear cluster in **51**. (b) Side view of the double calix[3]arene-shaped hexamer with polyanions.

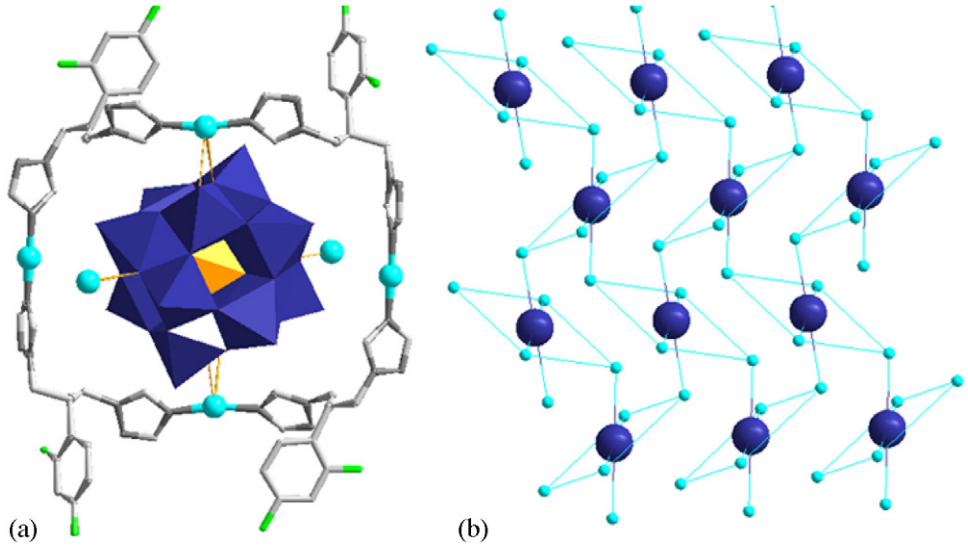

Fig. 16. (a) Ball-and-stick representation of the molecular square encapsulated polyhedral polyanion. (b) View of the stacking of the 2D structure of **52**.

the hexamers are arranged in a honeycomb-like structure with 1D hexagonal channels. The metal–organic cations and $[PMo_{12}O_{40}]^{3-}$ anions form a three-dimensional supramolecular network through weak N–H···O hydrogen bonds.

Compound **52** is composed of square tetranuclear copper oligomeric $[Cu^{I}_4(Hfcz)_4]^{4+}$ cations and $[SiW_{12}O_{40}]^{4-}$ polyanions [46]. The Cu(I) atoms are linked diagonally by the Hfcz ligands to form a square 40-membered ring in which a polyanion is contained. The polyanion exhibits a distorted structure and has weak coordination interactions with four Cu(I) metals through four terminal and two bridging O atoms, leading to a 2D structure as shown in Fig. 16.

3.3.2. *One-dimensional metal-triazole chains*

The structure of **53** consists of $[Ag_2(trz)_2]_n^{2n+}$ zigzag chains and γ-$[Mo_8O_{26}]_n^{4n-}$ anionic chains [45]. The Ag-trz chains are disposed in a face-to-face fashion with weak π–π interactions to form 2D Ag-trz layers. The γ-$[Mo_8O_{26}]^{4-}$ octamolybdate units are linked together through shared vertices to generate an infinite chain. The overall structure presents a layered ...ABAB... pattern (A = POM layer and B = Ag-trz layer) along the *b*-axis. The POM chains and the Ag-trz chains are essentially perpendicular with extensive hydrogen bonding between them (Fig. 17).

Complex **54** contains interesting cationic $[Ag_4(4atrz)_2Cl]_n^{3n+}$ looped chains and unprecedented anionic $[Ag(Mo_8O_{26})]_n^{3n-}$ chains [45,57]. In this compound, the 4atrz tridentate ligands link silver atoms to form 1D Ag-4atrz chains. The 1D chains are connected by $[Ag_2Cl]$ units to form looped chains (Fig. 18(a)). The anionic $[Ag(Mo_8O_{26})]_n^{3n-}$ chain in **54** is constructed from β-octamolybdate clusters and silver ions (Fig. 18(b)). The tetra-coordinated Ag^+ ion is sandwiched by two β-octamolybdate units. In the crystal packing, the POM chains and the Ag chains are essentially perpendicular.

Complexes **55** and **56** crystallize isostructurally and consist of one-dimensional Ag-1,2,4-triazole helix chains and Keggin anions (Fig. 19 (a) and (b)) [45]. The cationic helices and Keggin anions are linked by hydrogen bonds (N–H···O or C–H···O) to generate a three-dimensional organic-inorganic hybrid supramolecular host–guest structure (Fig. 19). The whole packing schemes of compounds **55** and **56** reveal a layered supramolecular structure (Fig. 19 (c)) in

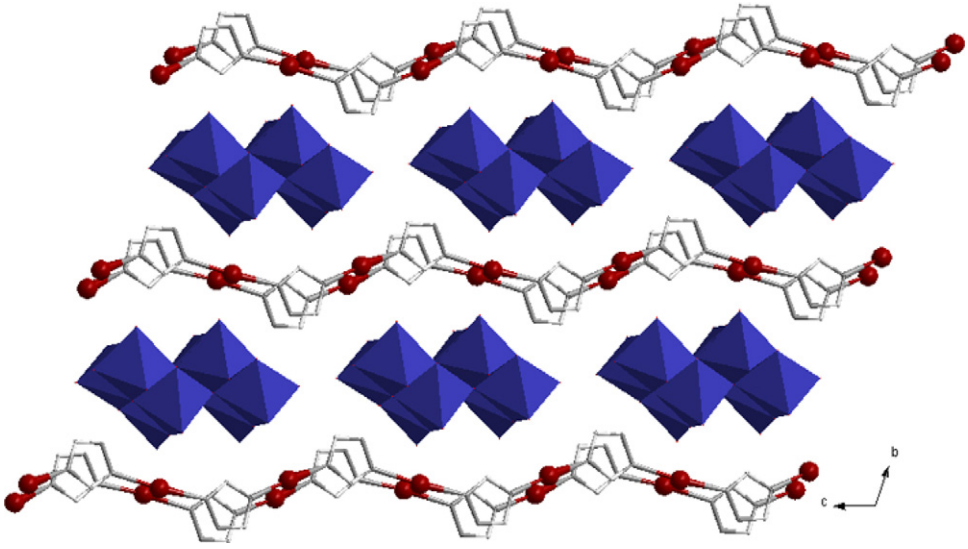

Fig. 17. View of structure **53** showing the layered structure and the extensive hydrogen bonding along the *a*-axis direction.

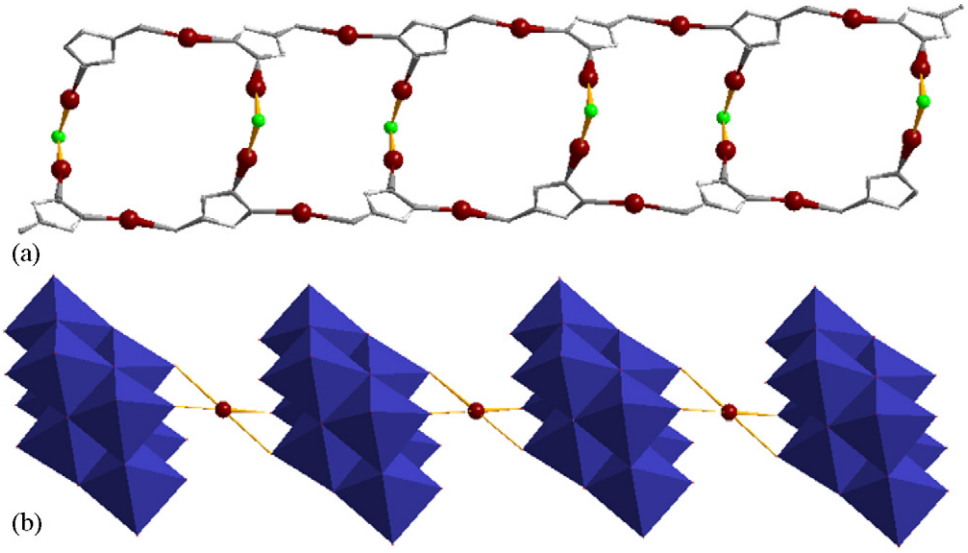

Fig. 18. (a) View of the looped chain in **54**. (b) Inorganic $[AgMo_8O_{26}]_n^{3n-}$ chain.

the . . .ABAB. . . mode (A = POM layer and B = Ag-trz layer) along the *a*-axis.

Compounds **57** and **58** are structural isomers [46]. They were prepared from the same starting materials but at different pH values. Their structures are composed of zigzag chains of $[Cu^I_2(Hfcz)_2]^{2+}$ and polyanions of $[SiW_{12}O_{40}]^{4-}$. Each Cu(I) is linearly coordinated by two Hfcz ligands. Hfcz ligands link Cu(I) cations in a bis(monodentate) mode to form the zigzag chains. Each $[SiW_{12}O_{40}]^{4-}$ polyanion has weak interactions with two Cu(I) ions from adjacent chains, leading to the formation of layers with 6^3 topology. However, the arrangements of the $[SiW_{12}O_{40}]^{4-}$ polyanions and the 1D chains in these compounds are different. Their structures are shown in Figs. 20 and 21.

Compound **62** is composed of 1D $[Cu(btb)]_n^{n+}$ chains and $[PMo_{12}O_{40}]^{3-}$ anions. Its packing structure is very interesting and can be viewed as being constructed from layers of 1D polymeric $[Cu(btb)]_n^{n+}$ chains and 2D $[Cu_2(btb)_2PMo_{12}O_{40}]_n^{n-}$ sheets (Fig. 22) [47]. The 2D sheets are constructed from 1D $[Cu(btb)]_n^{n+}$ chains and POMs through weak coordination interaction. Furthermore, the layers of 1D chains are linked through weak coordination Cu···O interactions (over 2.86 Å) into a layered 3D structure.

Compound **63** is constructed from a channel-like chain and $[SiMo_{12}O_{40}]^{4-}$ polyanions (Fig. 23) [48]. The 1D chains are first connected by the polyanions through weak coordination interaction to generate a 2D layer. Moreover, each polyanion also provides two terminal oxo groups to link Cu(I) atoms of the adjacent layers and thus fabricates the components into a 3D framework.

3.3.3. *Two-dimensional metal-triazole sheets*

The structures of compounds **64** and **65** are isomeric, which shows again the structural flexibility of coordination polymers. In compound **64** [49], four Cu (I) atoms are linked by four 1,2,4-triazole ligands with slightly distorted linear coordination into a cyclic $[Cu_4(trz)_4]$ tetramer. The adjacent tetramers are further linked by four Cu(I) atoms with linear coordination to form a 2D cationic network with square and octagonal motifs (Fig. 24(a)). From a topological viewpoint, this 2D sheet is a typical 4-connected 4^4 net with $[Cu_4(trz)_4]$ units as nodes and the remaining Cu^I ions as linkers. In

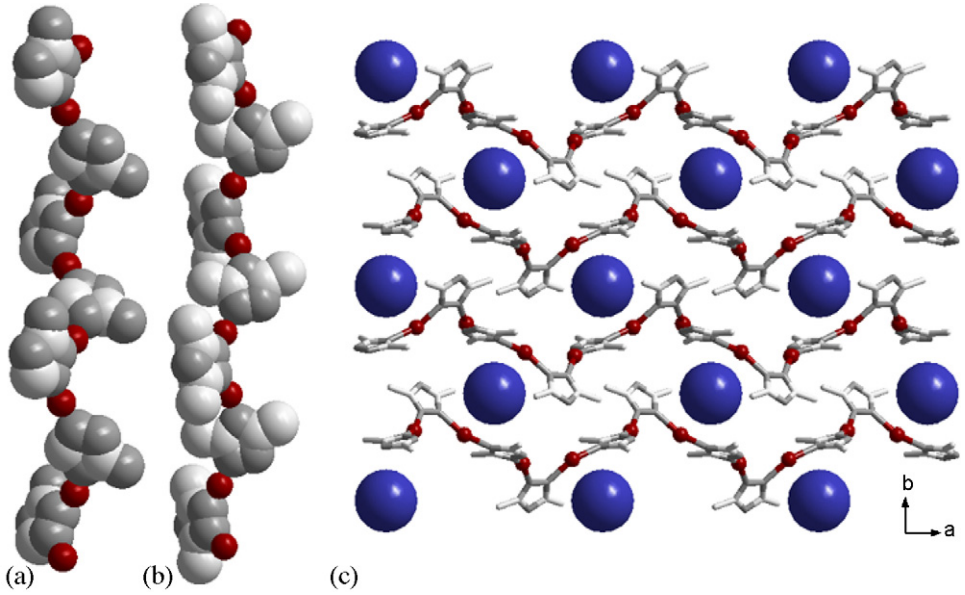

Fig. 19. Space-filling views of the helix chains in compounds **55** (a) and **56** (b), and the layered structure of **56** (c).

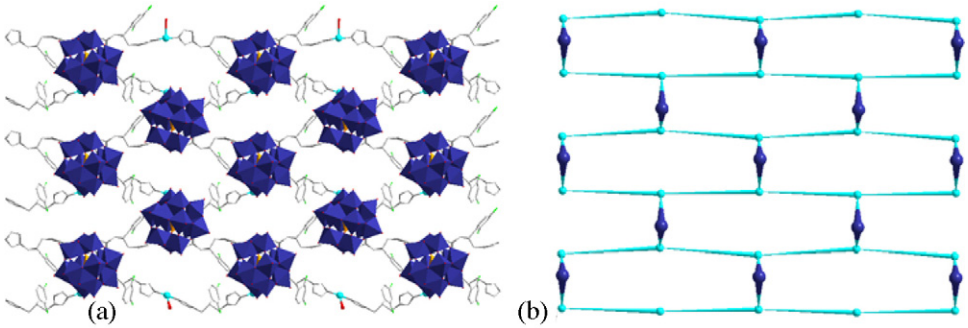

Fig. 20. Structure of **57**: (a) polyhedral and ball-and-stick representation; (b) schematic view of the 2D structure.

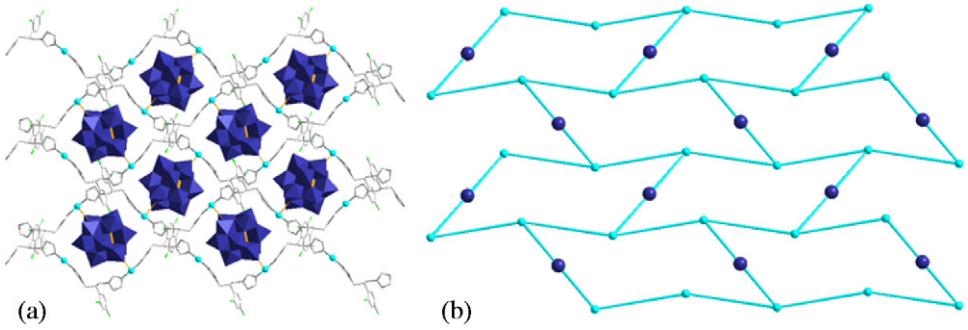

Fig. 21. Structure of **58**: (a) polyhedral and ball-and-stick representation; (b) schematic view of the 2D structure.

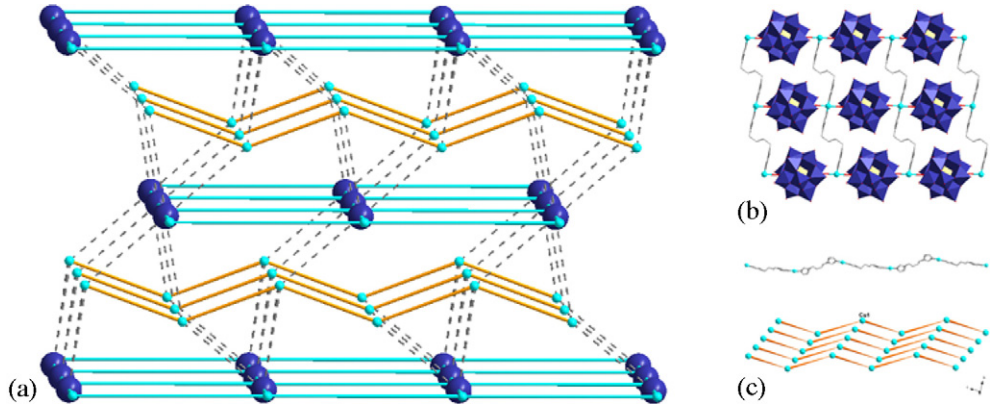

Fig. 22. Views of structure **62**: (a) the 1D $[Cu(btb)]_n^{n+}$ chains and 2D $[Cu_2(btb)_2PMo_{12}O_{40}]_n^{n-}$ sheets stack alternately into a layered structure. (b) The 2D $[Cu_2(btb)_2PMo_{12}O_{40}]_n^{n-}$ sheet. (c) The infinite wave-like chains.

compound **65**, the diagonal coordination of Cu(I) with the triazole ligand gives a $[Cu_3(trz)_3]$ trimer instead of a tetramer, as seen in **64** (Fig. 24(b)). The connection of each $[Cu_3(trz)_3]$ trimer with three adjacent ones by $[Cu_3(trz)]^{3+}$ units generates a 2D network with trigonal and nonagonal Cu-polygons. The Keggin $[PMo_{12}O_{40}]^{3-}$ anions are encapsulated in the octagon and nonagon in **64** and **65**, respectively. The parallel stacking of the 2D sheets in these compounds leads to layered structures as in **45** and **46**.

Compound **66** contains both coordinated and non-coordinated $[SiW_{12}O_{40}]^{4-}$ polyanions [50]. In this compound, each Co(II) atom is coordinated in a distorted octahedral geometry by four bridging Hfcz ligands, one water molecule, and one oxo group from a polyanion with Co–O distances of 2.184(8) Å. The Co(II) atoms are linked by Hfcz ligands in a bis(monodentate) bridging mode to generate $(4^4.6^2)$ sheets, which are further connected covalently by polyanions to form an interesting double layer. Such POM-sandwich sheets and layers of non-coordinated polyanions stack alternately into a 3D layered structure (Fig. 25).

3.3.4. *Three-dimensional metal-triazole polymers*

As was the case with pyrazine, non-tethered triazole ligands are also too small to construct homoleptic 3D coordination polymer/POM host–guest supramolecules. However, by using triazole derivatives with spacers, such supramolecules can be synthesized. For instance, compound **67** has an unusual polyoxometalate-encapsulated 3D polyrotaxane framework with molecular squares threading on a twofold interpenetrated diamondoid skeleton [51]. The compound is composed of a 3D network $[Cu^{II}(L)_2(H_2O)_2]^{2+}$ (L = 4,4′-bis(1,2,4-triazol-1-ylmethyl) biphenyl) (**A**), molecular square $[Cu^{I}_2(L)_2]^{2+}$(**B**), and Keggin anion

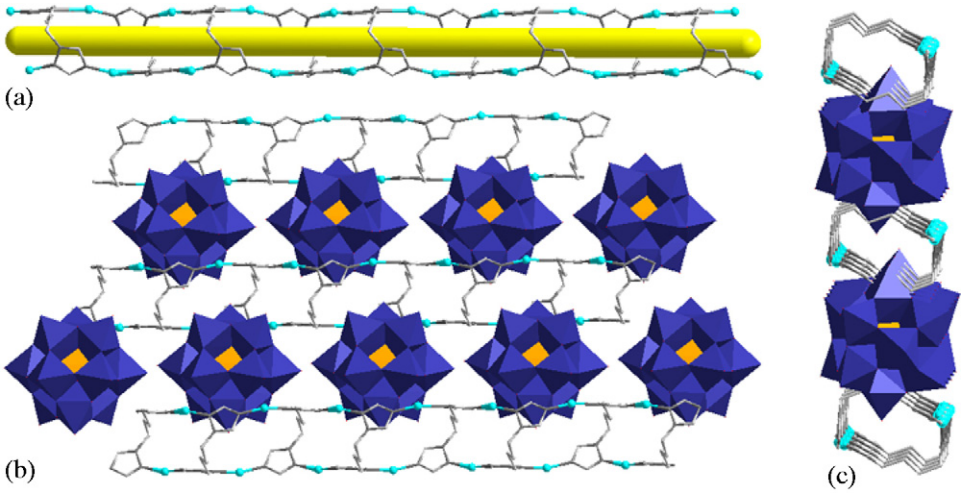

Fig. 23. (a) Channel-like chain in compound **63**. Chains and $[SiMo_{12}O_{40}]^{4-}$ anions are arranged alternately to construct a 2D layer viewed along (b) the *a*-axis and (c) the *c*-axis.

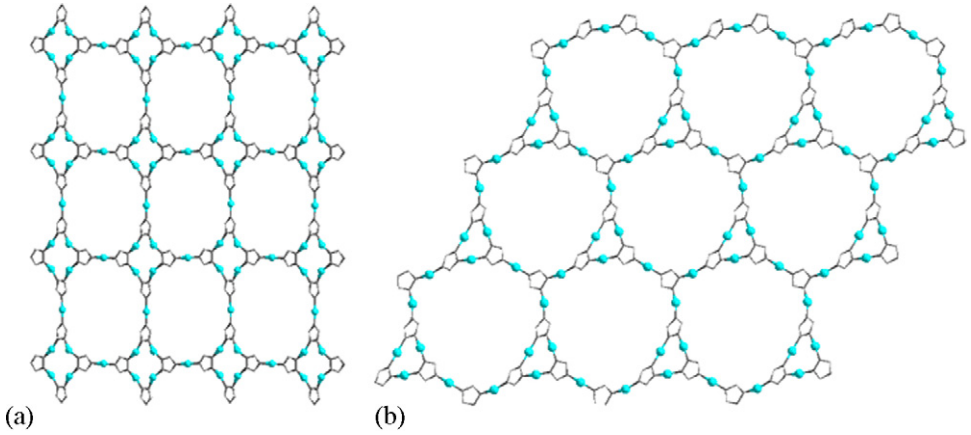

Fig. 24. The 2D metal organic cationic frameworks in **64** (a) and **65** (b).

$[PMo^{V}Mo^{VI}_{11}O_{40}]^{4-}$ (**C**). In fragment **A**, each Cu(II) center is linked to four adjacent metal centers through L ligands to form a typical diamondoid framework with large adamantanoid cage; two independent **A** fragments interpenetrate so as to effect efficient packing (Fig. 26). Furthermore, motif **B** and two **A** fragments are interlocked in such a way as to form a unique 3D [3]rotaxane with large voids in which fragment **C** is trapped.

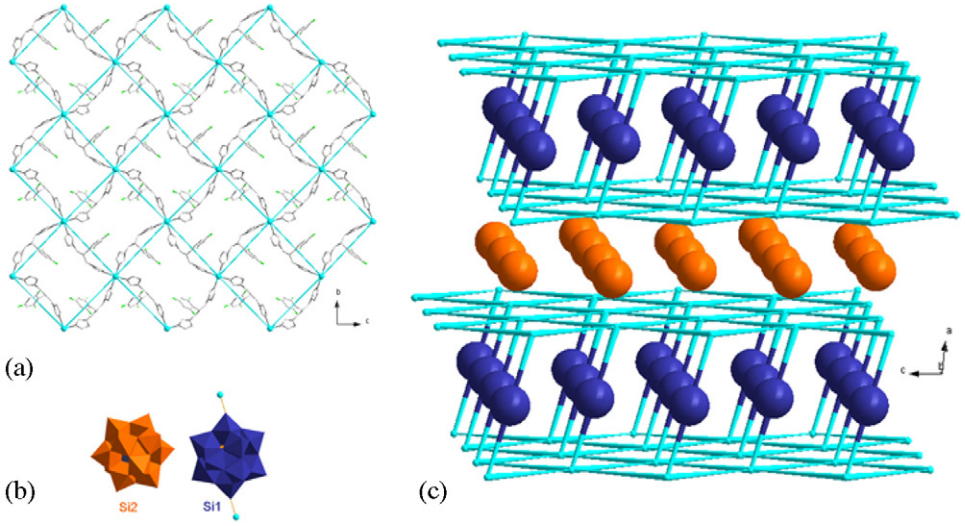

Fig. 25. Structure views of compound **66**: (a) metal–ligand 2D sheets; (b) two kinds of POM; (c) schematic structure of the crystal packing.

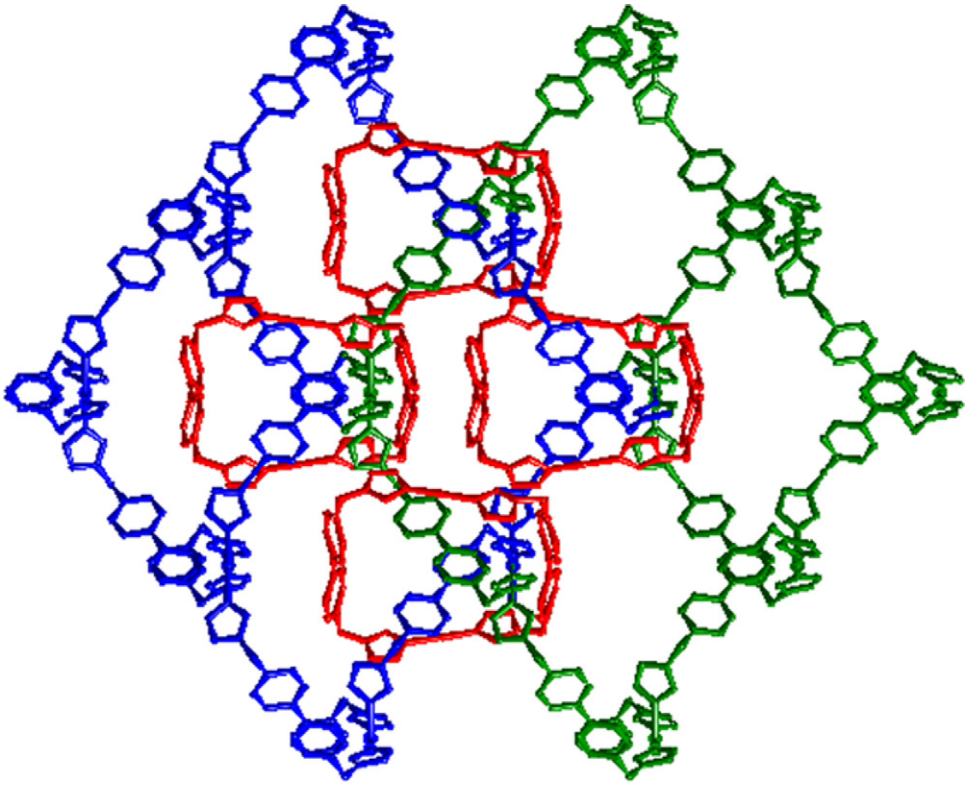

Fig. 26. Structure view of compound **67** showing interpenetrating diamondoid units locked by molecular squares.

3.4. PCPs/POM host–guest supramolecules constructed from imidazole ligands

Compounds **69**–**74** were synthesized from the same starting material at different pH values and metal–ligand stoichiometries under hydrothermal conditions [53,54]. The structures of these compounds demonstrate the dramatic influence of the reaction conditions, the metal–ligand stoichiometry and the weak interaction between the POM anions and the metal–organic framework upon the formation of these compounds. The structure of compound **69** is composed of 1D $[Cu(bbi)]_n^{n+}$ chains and two kinds of polyanions, $[\alpha\text{-}Mo_8O_{26}]^{4-}$ and $[\delta\text{-}Mo_8O_{26}]^{4-}$ [53]. In the structure, two 1D chains are linked alternately by $[\delta\text{-}Mo_8O_{26}]^{4-}$ and $[\alpha\text{-}Mo_8O_{26}]^{4-}$anions through Cu···O weak coordination to form a double-chain subunit. The double chains are further linked by 1D chains through the weak coordination of $[\alpha\text{-}Mo_8O_{26}]^{4-}$ anions and Cu(I) atoms into an 2D sheet with numerous cavities. Furthermore, additional isolated 1D chains penetrate the 2D sheet in an inclined way along the crystallographic *b*-axis to form a polythreaded structure, as shown in Fig. 27. Compound **70** is a supramolecular isomer of **69**, and its structure also has a polythreaded topology.

In **71**, the Cu(II) atoms are coordinated by four bridging bbi ligands to generate 2D coordination polymeric $[Cu(bbi)_2]_n^{2n+}$ layers. Adjacent layers are linked by $[\beta\text{-}Mo_8O_{26}]^{4-}$ polyanions through weak coordination interaction (Cu···O 2.732(4) Å) into a 3D framework α-Po topology (Fig. 28) [54]. Additional protonated bbi ligands act as counterions and are located in the channels of the 3D structure with extensive hydrogen bonding to the polyanions. In **72**, the Cu(II) atoms are coordinated by four bridging bbi ligands to generate 2D coordination polymeric $[Cu(bbi)_2]_n^{2n+}$ layers and afford a structure very similar to that in **71** [54]. The adjacent layers are also connected by $[\beta\text{-}Mo_8O_{26}]^{4-}$ polyanions through weak coordination interaction (Cu–O 2.511(4) Å), but only half of the Cu(II) centers in **72** are linked by the polyanions instead of all the Cu(II) atoms in **71**, leading to formation of a 3D framework with larger cavities. Two independent 3D frameworks interpenetrate one another in this structure.

Compounds **73** and **74** are supramolecular isomers [54]. Both structures consist of 1D $[Cu^{I}(bbi)]_n^{n+}$ chains, $[\alpha\text{-}Mo_8O_{26}]^{4-}$ polyan-

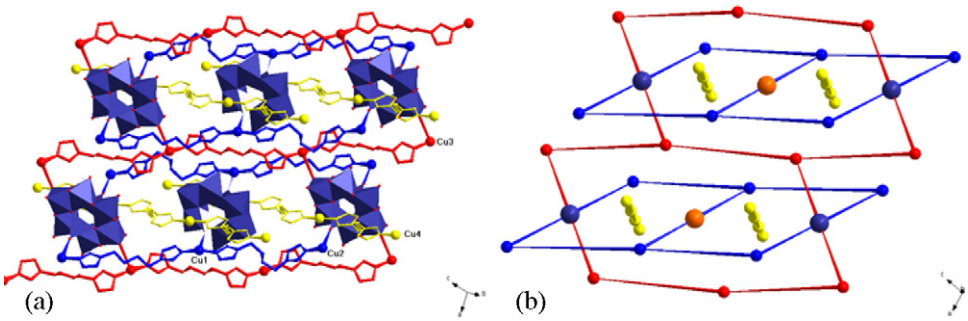

Fig. 27. View (a) and schematic representation (b) of the polythreaded structure **69**.

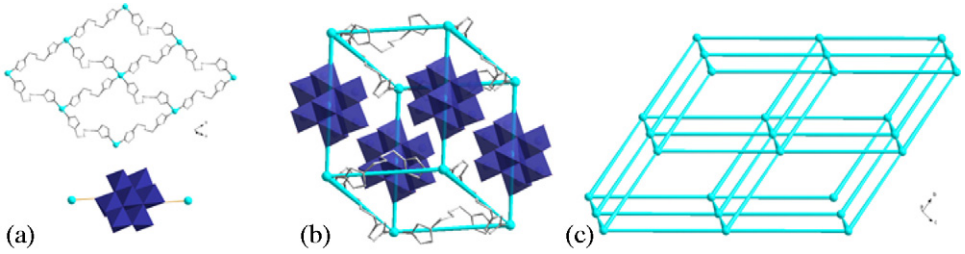

Fig. 28. Views of the structure **71** showing: (a) the 2D $[Cu(bbi)_2]_n^{2n+}$ metal–ligand sheet and $[\beta\text{-}Mo_8O_{26}]^{4-}$ polyanion. (b) The 3D framework built from the 2D sheets and polyanion. (c) Schematic view of the α-Po topology framework.

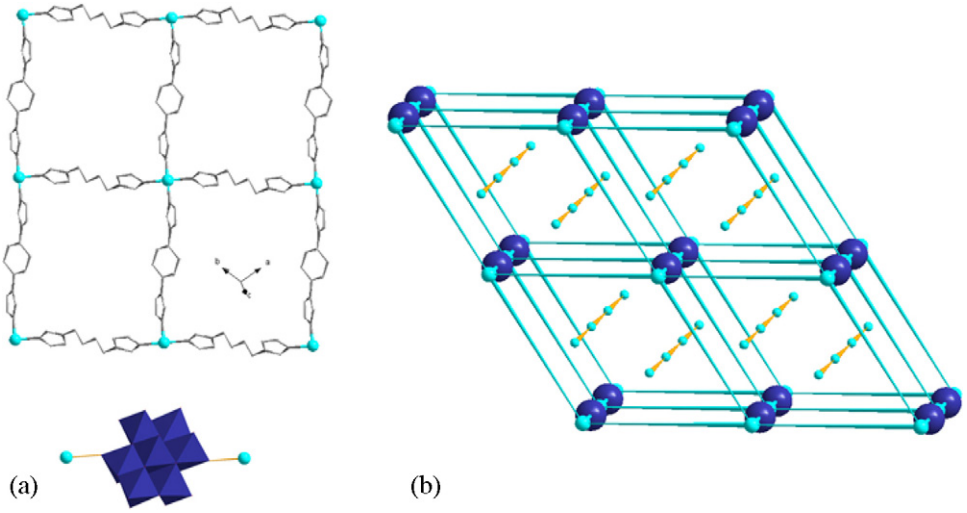

Fig. 29. Views of the structure **74**: (a) the 2D coordination polymer and $[\alpha\text{-}Mo_8O_{26}]^{4-}$ polyanion. (b) Schematic view of the 3D polythreaded framework.

ions and 2D metal–ligand sheets. In **73**, the combination of Cu(II) centers with bbi ligands generates 2D $[Cu^{II}(bbi)_2]_n^{2n+}$ layers, which are pillared by $[\alpha\text{-}Mo_8O_{26}]^{4-}$ polyanions (Cu···O 2.605(4) Å) and lead to the formation of a 3D framework with α-Po topology. The channels of the 3D framework are occupied by 1D $[Cu^{I}(bbi)]_n^{n+}$ chains, resulting in an unusual 3D polythreaded framework (Fig. 29). The 2D sheets in **75** contain both Cu(I) and Cu(II) ions. The Cu(I) ions are coordinated diagonally by two bridging bbi ligands, and the Cu(II) sites are coordinated by four bridging bbi ligands. The coordination of the Cu centers and bridging bbi ligands leads to 2D sheets with large 66-membered hexanuclear copper motifs. The Cu(II) centers further interact with the $[\alpha\text{-}Mo_8O_{26}]^{4-}$ polyanions (Cu···O 2.556(7) Å) to form a layer-pillared 3D framework with α-Po topology. The resulting channels contain 1D $[Cu^{I}(bbi)]_n^{n+}$ chains that form a polythreaded structure as in **73**. Weak coordination interaction exists between the 1D chains and the polyanions in compounds **73** and **74**.

4. Catalytic application of PCPs/POM host–guest supramolecules

In 2005, Férey and co-workers synthesized a chromium terephthalate-based porous coordination polymer MIL-101 with unusually large pore volumes and surface area [7a]. They also demonstrated that Keggin anions could be encapsulated inside the PCP in large amounts. The MIL-supported POM materials were assessed by Kholdeeva and co-workers as catalysts in the oxidation of three representative alkenes—α-pinene, caryophyllene, and cyclohexene—using molecular oxygen and aqueous hydrogen peroxide as oxidants [7b]. $NaH_3[PW_{11}Ti(OH)O_{39}]$ (Ti-POM)/MIL-101 and $[Bu_4N]_4H[PW_{11}Co(H_2O)O_{39}]$ (Co-POM)/MIL-101 have moderately good catalytic activity and selectivity in α-pinene allylic oxidation (81–84% verbonol/verbenone selectivity at 15–25% substrate conversion) and caryophyllene epoxidation with hydrogen peroxide (100% selectivity with 88% conversion) with the green oxidants H_2O_2 (Ti-POM) and O_2 (Co-POM). The Co-POM composite materials are stable to POM leaching, and can be used repeatedly without sustaining a loss of activity and selectivity in oxidations with O_2. Under mild reaction conditions ($T < 50\,^{\circ}C$, $[H_2O_2] < 0.2$ M), Ti-POM is rather stable, does not undergo catalyst leaching, and can be recycled with no loss of catalytic properties.

By using a reported porous coordination polymer complex, $[Cu_3(TMA)_2(H_2O)_3]_n$ (TMA = deprotonated trimesic acid = 1,3,5-benzenetricarboxylate) as host [58], the Yamase and Liu groups have synthesized a series of PCP/POM host–guest composite materials, POM = $[H_2SiW_{12}O_{40}]^{2-}$ (**75**); $[H_2GeW_{12}O_{40}]^{2-}$ (**76**); $[HPW_{12}O_{40}]^{2-}$ (**77**); $[H_2SiMo_{12}O_{40}]^{2-}$ (**78**); $[HPMo_{12}O_{40}]^{2-}$ (**79**); $[HAsMo_{12}O_{40}]^{2-}$ (**80**) [7c,59]. X-ray single-crystal analysis indicates that only about half of the pores in the host are occupied by polyanions and that the empty pores remain available to host other species. The latter group used compound **77** in catalytic hydrolysis of esters in excess water [7c]. The catalytic activity of this compound in hydrolysis reactions is size selective. With smaller esters like methyl esters and ethyl esters, very high catalytic activity was observed. Moreover, the catalyst behaves in completely heterogeneous fashion and can be recycled 15 times without loss of reactivity and selectivity. No POM leaching was observed.

5. Conclusion

In summary, significant progress has been reported in the synthesis and structural study of PCPs/POM host–guest composite

materials over the last two decades. Much effort has been devoted to the synthesis of materials under the template effect of discrete POMs, such as $M_6O_{19}^{n-}$, $XM_{12}O_{40}^{n-}$, $X_2M_{18}O_{62}^{n-}$, and $Mo_8O_{26}^{4-}$. PCPs/POM host–guest composite materials of diverse topologies can be prepared using simple reaction techniques. The structures of the materials can be easily tuned by adjusting the reaction conditions, the metal–ligand stoichiometry, the template polyanions, and the co-ligand, thus allowing for a rational engineering of such materials. Even though still in their infancy, PCPs/POM materials have shown promising results for some organic transformations. However, the applications of these materials still remain largely unexplored. The next stage of research in this area should be function-oriented. Introduction of enantiopure host or guest molecules into these materials remains to be done. Another exciting and challenging effort in this area is the removal POM anions without decomposition of the overall 3D framework. If POM anions could be substituted by free counteranions, these materials might be useful for anion-exchange.

Acknowledgments

This work was supported by the 973 key program of the MOST (2006CB932904, 2007CB815304), the National Natural Science Foundation of China (20425313, 20873150, 20821061, and 50772113), the Chinese Academy of Sciences (KJCX2-YW-M05), and the Fund of Fujian Key Laboratory of Nanomaterials (2006L2005). Support from the National Science Foundation (Grant CHE-0845829) to J.P.D. is gratefully acknowledged.

References

[1] (a) Special issue on polyoxometalate. Chem. Rev. 98 (1998) 1 and reference therein;
(b) M.T. Pope, A. Müller (Eds.), Polyoxometalate Chemistry; From Topology via Self-Assembly to Application, Kluwer Academic, Dordrecht, The Netherlands, 2001;
(c) C.L. Hill, C.M. Mccartha, Coord. Chem. Rev. 143 (1995) 407;
(d) M.T. Pope, A. Müller, Angew. Chem. Int. Ed. Engl. 30 (1991) 34;
(e) M.T. Pope, Inorg. Chem. 11 (1972) 1973.

[2] (a) A. Müller, S. Roy, Coord. Chem. Rev. 245 (2003) 153;
(b) A. Müller, D. Rehder, E.T.K. Haupt, A. Merca, H. Bogge, M. Schmidtmann, G.H. Bruckner, Angew. Chem. Int. Ed. 43 (2004) 4466;
(c) C. Ritchie, C. streb, J. Thiel, S.G. Mitchell, H.N. Miras, D.L. Long, T. Boya, R.D. Peacock, T.M. Glone, L. Cronin, Angew. Chem. Int. Ed. 47 (2008) 6881;
(d) J. Thiel, C. Ritchie, C. Streb, D.L. Long, L. Cronion, J. Am. Chem. Soc. 131 (2009) 4180;
(e) F. Hussain, B.S. BAssil, L.H. Bi, M. Reicke, U. Kortz, Angew. Chem. Int. Ed. 43 (2004) 3585;
(f) S. Sankar, U. Kortz, Angew. Chem. Int. Ed. 44 (2005) 3777;
(g) N.L. Laronze, M. Haouas, J. Marrot, F. Taulette, G. Herve, Angew. Chem. Int. Ed. 45 (2006) 139;
(h) M.N. Sokolov, I.V. Kalinina, E.V. Peresypkina, E. Cadot, S.V. Takchev, V.P. Fedin, Angew. Chem. Int. Ed. 47 (2008) 1467;
(i) H.N. Miras, J. Yan, D.L. Long, L. Cronin, Angew. Chem. Int. Ed. 47 (2008) 8420.

[3] (a) S.T. Zheng, J. Zhang, G.Y. Yang, Angew. Chem. Int. Ed. 47 (2008) 3909;
(b) C.D. Wu, C.Z. Lu, H.H. Zhuang, J.S. Huang, J. Am. Chem. Soc. 124 (2002) 3836;
(c) C. Fleming, D.L. Long, L. Cronin, Nature Nanotechnol. 3 (2008) 229;
(d) D. Attanasio, F. Bachechi, Adv. Mater. 6 (1994) 145;
(e) D.L. Long, E. Burkholder, L. Cronin, Chem. Soc. Rev. 36 (2007) 105;
(f) S. Uchida, M. Hashimoto, N. Mizuno, Angew. Chem. Int. Ed. 41 (2002) 2814;
(g) J.W. Zhao, J. Zhang, S.T. Zheng, G.Y. Yang, Chem. Commun. 2008 (2008) 570;
(h) W. Yang, C. Lu, X. Lin, H. Zhuang, Inorg. Chem. 41 (2002) 452;
(i) W. Chen, Y. Li, Y. Wang, E. Wang, Z. Zhang, Dalton Trans. 2008 (2008) 865.

[4] (a) A. Proust, R. Thouvenot, P. Gouzerh, Chem. Commun. 2008 (2008) 1837;
(b) Z.W. Xi, N. Zhou, Y. Sun, K.L. Li, Science 292 (2001) 1139;
(c) K. Sato, M. Aoki, R. Noyori, Science 281 (1998) 1646;
(d) R. Noyori, M. Aoki, K. Sato, Chem. Commum. 2003 (2003) 1977;
(e) N. Mizuno, K. Yamaguchi, K. Kamata, Coord. Chem. Rev. 249 (2005) 1944;
(f) K. Kamata, Y. Nakagawa, N. Mizuno, J. Am. Chem. Soc. 130 (2008) 15304;
(g) Y. Kikukawa, S. Yamaguchi, N. Mizuno, J. Am. Chem. Soc. 130 (2008) 15872;
(h) H. Hamamoto, Y. Suzuki, S. Ikegami, Angew. Chem. Int. Ed. 44 (2005) 4536;
(i) J. Gao, Y. Zhang, C. Li, Chem. Commun. 2008 (2008) 332;
(j) Y.V. Geletii, B. Botar, C.L. Hill, Angew. Chem. Int. Ed. 47 (2008) 3896;
(k) C.M. Roch, C.R. Mayer, A. Michel, E. Dumas, F.X. Liu, Chem. Commun. (2007) 3750;
(l) P. Romero, Adv. Mater 13 (2001) 163;
(m) I.V. Kozhevnikov, Catalysts for Fine Chemicals, vol. 2, Catalysis by Polyoxometalates, Wiley, Chichester, UK, 2002;
(n) N. Mizuno, M. Misono, Chem. Rev. 98 (1998) 199;
(o) C.L. Hill, J. Mol. Catal. A: Chem. 262 (2007) 2.

[5] (a) Y. Guo, C. Hu, J. Mol. Catal. A 262 (2007) 136;
(b) R.D. Gall, C.L. Hill, J.E. alker, Chem. Mater. 8 (1996) 2523;
(c) B.A. Watson, M.A. Barteau, L. Haggerty, A.M. Lenhoff, R.S. Weber, Langmuir 8 (1992) 1145;
(d) M.A. Schwegler, H. Van Bekkum, N.A. de Munck, Appl. Catal. 74 (1991) 191;
(e) C.T. Kresge, M.E. Leonowicz, W.J. Roth, J.C. Vartuli, J.S. Beck, Nature 359 (1992) 710;
(f) D. Zhao, J. Feng, Q. Huo, N. Melosh, G.H. Fredrickson, B.F. Chmelka, G.D. Stucky, Science 279 (1998) 548;
(g) B.J.S. Johnson, A. Stein, Inorg. Chem. 40 (2001) 801;
(h) R.J. Errington, S.S. Petkar, B.R. Horrocks, A. Houlton, L.H. Lie, S.N. Patole, Angew. Chem. Int. Ed. 44 (2005) 1254;
(i) R. Neumann, H. Miller, J. Chem. Soc. Chem. Commun. (1995) 2277;
(j) W. Kaleta, K. Nowinska, Chem. Commun. (2001) 535;
(k) O.A. Kholdeeva, M.P. Vanina, M.N. Timofeeva, R.I. Maksimovskaya, T.A. Trubitsina, M.S. Melgunov, E.B. Burgina, J. Mrowiec-Bialon, A.B. Jarzebski, C.L. Hill, J. Catal. 226 (2004) 363;
(l) M.V. Vasylyev, R. Neumann, J. Am. Chem. Soc. 126 (2004) 884;
(m) J. Kasai, Y. Nakagawa, S. Uchida, K. Yamaguchi, N. Mizuno, Chem. Eur. J. 12 (2006) 4176.

[6] (a) S. Kitagawa, R. Matsuda, Coord. Chem. Rev. 222 (2007) 2490;
(b) H.K. Chae, O.M. Yaghi, Nature 427 (2005) 523;
(c) D.J. Tranchemontagne, N. Zheng, M. O'Keeffe, O.M. Yaghi, Angew. Chem. Int. Ed. 47 (2008) 5136;
(d) M.O. Keeffe, M.A. Peskov, S.J. Ramsden, O.M. Yaghi, Acc. Chem. Res. 41 (2008) 1782;
(e) H. Zhao, Z.R. Qu, H.Y. Ye, R.G. Xiong, Chem. Soc. Rev. 37 (2008) 84;
(f) M. Oh, G.B. Garpentar, D.A. Sweigart, Acc. Chem. Res. 37 (2004) 1;
(g) J.R. Nitschke, Acc. Chem. Res. 40 (2007) 103;
(h) X.M. Chen, T.L. Tong, Acc. Chem. Res. 40 (2007) 162;
(i) L.R.M. Gillivray, G.S. Papaefstathiou, T. Friscic, T.D. Hamilton, T.D. Hamilton, D.K. Bucar, Q. Chu, D.B. Varshney, I.G. Georgiev, Acc. Chem. Res. 41 (2008) 280;
(j) J.A. Thomas, Chem. Soc. Rev. 36 (2007) 856;
(k) T. Kudernac, S. Lei, J.A.A.W. Elemans, S.D. Feyter, Chem. Soc. Rev. 38 (2009) 402;
(l) J.W. Lauher, F.W. Fowler, N.S. Goroff, Acc. Chem. Res. 41 (2008) 1215;
(m) X.H. Bu, M.L. Tong, H.C. Chang, S. Kitagawa, S.R. Batten, Angew. Chem. Int. Ed. 43 (2004) 192.

[7] (a) G. Férey, C. Mellot-Draznieks, C. Serre, F. Millange, J. Dutour, S. Surble, I. Margiolaki, Science 309 (2005) 2040;
(b) N.V. Maksimchuk, M.N. Timofeeva, M.S. Melgunov, A.N. Shmakov, Yu.A. Chesalov, D.N. Dybtsev, V.P. Fedin, O.A. Kholdeeva, J. Catal. 257 (2008) 315;
(c) C.Y. Sun, S.X. Liu, D.D. Liang, K.Z. Shao, Y.H. Ren, Z.M. Su, J. Am. Chem. Soc. 131 (2009) 1883.

[8] (a) R.C. Haushalter, K.G. Strohmaier, F.W. Lai, Science 246 (189) 1989;
(b) R.C. Haushalter, L.A. Mundi, Chem. Mater. 4 (1992) 31;
(c) M.I. Khan, L.M. Meyer, R.C. Haushalter, C.L. Schweitzer, J. Zubieta, J.L. Dye, Chem. Mater. 8 (1996) 43.

[9] P.H. Hagrman, D. Hagrman, J. Zubieta, Angew. Chem. Int. Ed. 38 (1999) 2638.

[10] (a) M. Sadakane, M.H. Dickman, M. Pope, Angew. Chem. Int. Ed. 39 (2000) 2914;
(b) R.C. Howell, F.G. Perez, S.J. William Dew, L.C. Francesconi, Angew. Chem. Int. Ed. 40 (2001) 4031;
(c) K. Fukaya, T. Yamase, Angew. Chem. Int. Ed. 42 (2003) 654;
(d) U. Kortz, M. Reicke, F. Hussain, Angew. Chem. Int. Ed. 44 (2005) 3733;
(e) X.K. Fang, P. Kögerler, Angew. Chem. Int. Ed. 47 (2008) 8123;
(f) C. Ritchie, G.J.T. Copper, Y.F. Song, C. Streb, H. Yin, A.D.C. Parenty, D.A. Maclaren, J. Cronin, Nat. Chem. 1 (2009) 47.

[11] (a) A. Müller, E. Beckmann, H. Bogge, M. Schmidtmann, A. Dress, Angew. Chem. Int. Ed. 41 (2002) 1162;
(b) J. Schemberg, A. Müller, U. Ermler, Angew. Chem. Int. Ed. 46 (2007) 2408.

[12] D.L. Long, H. Abbas, P. Kögerler, L. Cronin, Angew. Chem. Int. Ed. 44 (2005) 3415.

[13] (a) K. Kamata, Y. Sumida, K. Yamaguchi, S. Hikichi, N. Mizuno, Science 300 (2003) 964;
(b) G.J. Rivera, J.A. Dumesic, Science 305 (2004) 1280;
(c) A.M. Khenkin, R. Neumann, J. Am. Chem. Soc. 124 (2002) 4198;
(d) N.M. Okun, T.M. Anderson, C.L. Hill, J. Am. Chem. Soc. 125 (2003) 3194;
(e) B. Botar, Y.V. Geletii, P. Kögerler, D.G. Musaev, C.L. Hill, J. Am Chem. Soc. 128 (2006) 11268;
(f) J. Macht, M.J. Jaink, M. Neurock, E. Iglesia, Angew. Chem. Int. Ed. 46 (2007) 7864;
(g) Y. Leng, J. Wang, D. Zhu, X. Ren, Angew. Chem. Int. Ed. 48 (2009) 168.

[14] (a) D.E. Katsoulis, Chem. Rev. 98 (1998) 359;
(b) T. Yamase, Chem. Rev. 98 (1998) 307;
(c) L. Chen, F. Jiang, Z. Lin, Y. Zhou, C. Yue, M. Hong, J. Am. Chem. Soc. 127 (2005) 8588.

[15] (a) D.L. Long, L. Cronin, Chem. Eur. J. 12 (2006) 3698;
(b) R.Y. Wang, D.Z. Jia, L. Zhang, Z.P. Guo, B.Q. Li, J.X. Wang, Adv. Funct. Mater. 16 (2006) 687;
(c) M. Alam, Y.S. Kim, S. Ogawa, A. Tsuda, N. Ishii, T. Aida, Angew. Chem. Int. Ed. 47 (2008) 2070.

[16] T. Yamase, J. Mater. Chem. 15 (2005) 4773.

[17] (a) E. Coronado, C.J. Garcia, Chem. Rev. 98 (1998) 273;
(b) G. Férey, C. Draznieks, C. Serre, F. Millange, Science 309 (2005) 2040;
(c) E. Coronado, J. Mascarós, C. Saiz, Adv. Mater. 16 (2004) 324;
(d) C. Jiang, A. Lesban, R. Kawamoto, S. Uchida, N. Mizuno, J. Am. Chem. Soc. 128 (2006) 14240;
(e) A.M. Douvas, E. Makarona, N. Glezos, P. Argitis, ACS Nano. 2 (2008) 733.
[18] (a) J.T. Rhule, C.L. Hill, Chem. Rev. 98 (1998) 327;
(b) D.A. Judd, J.H. Nettles, N. Nevins, J.P. Snyder, D.C. Liotta, J. Tang, J. Ermolieff, R.F. Schinazi, C.L. Hill, J. Am. Chem. Soc. 123 (2001) 886.
[19] (a) C.Z. Lu, C.D. Wu, S.F. Lu, J.C. Liu, Q.J. Wu, H.H. Zhuang, J.S. Huang, Chem. Commun. 2002 (2002) 152;
(b) P. Mialane, C. Duboc, J. Marrot, E. Rivière, Chem. Eur. J. 12 (2006) 1950;
(c) L. Lisnard, P. Mialane, A. Dolbecq, J.M. Juan, L. Nadjo, Chem. Eur. J. 13 (2007) 3525;
(d) C. Ritchie, A. Ferguson, H. Nojiri, H. Miras, Y.F. Song, D.L. Long, L. Cronin, Angew. Chem. Int. Ed. 47 (2008) 5609.
[20] (a) P. Gouzerh, A. Proust, Chem. Rev. 98 (1998) 77;
(b) Z.H. Peng, Angew. Chem. Int. Ed. 43 (2004) 930;
(c) P. Mialane, A. Dolbecq, F. Secheresse, Chem. Commun. (2006) 3477.
[21] S.I. Noro, S. Kitagawa, T. Akutagawa, T. Nakamura, Prog. Polymer Sci. 34 (2009) 240.
[22] D. Tanaka, S. Kitagawa, Chem. Mater. 20 (2008) 922.
[23] X.J. Kong, Y.P. Ren, P.Q. Zheng, Y.X. Long, L.S. Long, Inorg. Chem. 45 (2006) 10702.
[24] P.Q. Zheng, Y.P. Ren, L.S. Long, R.B. Huang, L.S. Zheng, Inorg. Chem. 44 (2005) 1190.
[25] K. Uehare, K. Kasai, N. Mizuno, Inorg. Chem. 46 (2007) 2563.
[26] D. Hagrman, C. Zubieta, D.J. Rose, J. Zubieta, R.C. Haushalter, Angew. Chem. Int. Ed. Engl. 36 (1997) 873.
[27] H. Jin, Y. Qi, E. Wang, Y. Li, C. Qin, X. Wang, S. Chang, Eur. J. Inorg. Chem. (2006) 4541.
[28] L. San Felices, P. Vitoria, J.M. Gutierrez-Zorrilla, L. Lezama, R.S. Einoso, Inorg. Chem. 45 (2006) 7748.
[29] J. Sha, J. Peng, A.X. Tian, H.S. Liu, J. Chen, P.P. Zhang, Z.M. Su, Cryst. Growth Des. 7 (2007) 2535.
[30] Y. Wang, D.R. Xiao, L.F. Fan, E.B. Wang, J. Liu, J. Mol. Struct. 843 (2007) 87.
[31] L. Yuan, C. Qin, X. Wang, E. Wang, S. Chang, Eur. J. Inorg. Chem. (2008) 4936.
[32] P.Q. Zheng, Y.P. Ren, L.S. Long, R.B. Huang, L.S. Zheng, Inorg. Chem 44 (2005) 1190.
[33] Y. Wang, D.R. Xiao, E.B. Wang, L.L. Fan, J. Liu, Trans. Met. Chem. 32 (2007) 950.
[34] K. Uehara, H. Nakao, R.K. awamoto, S. Hikichi, N. Mizuno, Inorg. Chem. 45 (2006) 9448.
[35] W.M.L. ei, C. He, Q.Z. Sun, Q.J. Meng, C.Y. Duan, Inorg. Chem. 46 (2007) 5957.
[36] C.Y. Sun, Y.G. Li, E.B. Wang, D.R. Xiao, H.Y. An, L. Xu, Inorg. Chem. 46 (2007) 1563.
[37] Y.G. Li, L.M. Dai, Y.H. Wang, X.L. Wang, E.B. Wang, Z.M. Sun, L. Xu, Chem. Commun. (2007) 2593.
[38] C. Inman, J.M. Knaust, S.W. Keller, Chem. Commun. (2002) 156.
[39] X.Y. Zhao, D.D. Liang, S.X. Liu, C.Y. Sun, R.G. Cao, C.Y. Gao, Y.H. Ren, Z.M. Su, Inorg. Chem. 47 (2008) 7133.
[40] X. Wang, Y. Bi, B. Chen, H. Lin, G. Liu, Inorg. Chem. 47 (2008) 2442.
[41] D. Hagrman, P.J. Hagrman, J. Zubieta, Angew. Chem. Int. Ed. Engl. 38 (1999) 3165.
[42] C.H. Li, K.L. Huang, Y.N. Chi, X. Liu, Z.G. Han, L. Shen, C.W. Hu, Inorg. Chem. 48 (2009) 2010.
[43] L.-M. Zheng, Y. Wang, X. Wang, J.D. Korp, A.J. Jacobson, Inorg. Chem. 40 (2001) 1380.
[44] L. Wang, X.P. Sun, M.L. Liu, Y.Q. Gao, W. Gu, X. Liu, J. Cluster Sci. 19 (2008) 531.
[45] Q.G. Zhai, X.Y. Wu, S.M. Chen, Z.G. Zhao, C.Z. Lu, Inorg. Chem. 46 (2007) 5046.
[46] S.L. Li, Y.Q. Lan, J.F. Ma, J. Yang, J. Liu, Y.M. Fu, Z.M. Su, Dalton Trans. (2008) 2015.
[47] A.X. Tian, J. Ying, J. Peng, J.Q. Sha, H.J. Pang, P.P. Zhang, Y. Chen, M. Zhu, Z.M. Su, Cryst. Growth Des. 8 (2008) 3717.
[48] A.X. Tian, J. Ying, J. Peng, J.Q. Sha, H.J. Pang, P.P. Zhang, Y. Chen, M. Zhu, Z.M. Su, Inorg. Chem. 48 (2009) 100.
[49] Q.G. Zhai, X.Y. Wu, S.M. Chen, Z.G. Zhao, C.Z. Lu, Inorg. Chim. Acta 360 (2007) 3484.
[50] Y.Q. Lan, S.L. Li, K.Z. Shao, X.L. Wang, Z.M. Su, Dalton Trans. (2008) 3824.
[51] X.L. Wang, C. Qin, E.B. Wang, Z.M. Su, Chem. Commun. (2007) 4245.
[52] B.X. Dong, J. Peng, P.P. Zhang, A.X. Tian, J. Chen, B. Xue, Inorg. Chem. Commun. 10 (2007) 839.
[53] Y.Q. Lan, X.L. Li, K.Z. Wang, Z.M. Shao, E.B. Su, Wang, Inorg. Chem. 47 (2008) 529.
[54] Y.Q. Lan, S.L. Li, X.L. Wang, K.Z. Shao, D.Y. Du, H.Y. Zang, Z.M. Su, Inorg. Chem. 47 (2008) 8179.
[55] (a) M. Fujita, K. Ogura, Bull. Chem. Soc. Jpn. 69 (1996) 1471;
(b) P.J. Stang, B. Olenyuk, Acc. Chem. Res. 30 (1997) 502.
[56] (a) M. Fujita, J. Yazaki,.K. Ogura, Tetrahedron Lett. 32 (1991) 5589;
(b) S.B. Lee, S. Hwang, D.S. Chung, H. Yun, J.-I. Hong, Tetrahedron Lett. 39 (1998) 873;
(c) M. Willemann, C. Mulcahy, R.K.O. Sigel, M.M. Cerdaĭ, E. Freisinger, P.J.S. Miguel, M. Roitzsch, B. Lippert, Inorg. Chem. 45 (2006) 2093.
[57] (a) C. Streb, C. Ritchie, D.L. Long, P. Kögerler, L. Cronin, Angew. Chem. Int. EP. 46 (2007) 7579;
(b) H. Abbas, C. Streb, A.L. Pickering, A.R. Neil, D.L. Long, L. Cronin, Cryst. Growth Des. 8 (2008) 636;
(c) E.F. Wilson, H. Abbas, B.J. Duncombe, C. Streb, D.L. Long, L. Cronin, J. Am. Chem. Soc. 130 (2008) 13878.
[58] S.S.Y. Chui, S.M.F. Lo, J.P.H. Chamant, A.G. Orpen, I.D. Williams, Science 283 (1999) 1148.
[59] L. Yang, H. Naruke, T. Yamase, Inorg. Chem. Commun. 6 (2003) 1020.